DEPARTMENT OF MECHANICAL AND INDUSTRIAL ENGINEERING
LABORATORY FOR ERGONOMICS RESEARCH
ENGINEERING EXPERIMENT STATION
UNIVERSITY OF ILLINOIS AT URBANA - CHAMPAIGN
URBANA, ILLINOIS 61801

STEADY STATE AND TRANSIENT TEMPERATURE DISTRIBUTIONS IN THE HUMAN THIGH COVERED WITH A COOLING PAD

by

R. J. LEO
A. SHITZER
J. C. CHATO
B. A. HERTIG

Technical Report No. ME-TR-286
June 1971

Supported by
National Aeronautics and Space Administration
under
Grant No. NGR-14-005-103

STEADY STATE AND TRANSIENT TEMPERATURE DISTRIBUTIONS IN THE HUMAN THIGH COVERED WITH A COOLING PAD

by

R. J. Leo
A. Shitzer
J. C. Chato
B. A. Hertig

Technical Report No. ME-TR-286

June 1971

Supported by

National Aeronautics and Space Administration

under

Grant No. NGR 14-005-103

ABSTRACT

An analytical and experimental study was done on the performance of cooling pads attached to a human thigh. Each cooling pad consisted of a long, water cooled tube formed into a serpentine shape with uniform spacing between the parallel sections.

The analytical work developed a cylindrical model for the human thigh. The transient times predicted by this model ranged from 25 to 80 minutes, which is reasonably close to the experimental results. Calculated and measured steady state temperature profiles were in fair agreement.

Three cooling pads with different cooling tube sizes and spacings were constructed and tested. These pads were equipped with thermocouples to measure the temperature profiles between adjacent tubes on the skin surface of a thigh of a male subject while he was performing various activity schedules. The pad with the highest tube density removed the greatest amounts of heat with the least temperature variations on the skin. Also, the transient times for this pad were the shortest.

The transient times associated with a change from a high metabolic rate of 1800 Btu/hr (528 w) to a low level of 300 Btu/hr (88 w), were found to be about 120 minutes. A change from 900 Btu/hr (264 w) to 300 Btu/hr (88 w) resulted in 90 to 100 minute transients. However, the transient times for a change in metabolic rate in the opposite direction from 300 Btu/hr (88 w) to 1800 Btu/hr (528 w) were 40 to 60 minutes. When an intermediate step of 900 Btu/hr (264 w) was introduced between the last two metabolic rates, the transient times associated with the individual steps varied from 40 to 80 minutes. However, the overall transient times for each double step were approximately the same in either direction.

NOMENCLATURE†

a	half distance between cooling tubes, [L]
A	total skin surface area, $[L^2]$
b	depth of tissue layer, [L]
c_b	specific heat of blood, $[L^2\theta^{-2}T^{-1}]$ or $[QM^{-1}T^{-1}]$
c_p	specific heat of tissue, $[L^2\theta^{-2}T^{-1}]$ or $[QM^{-1}T^{-1}]$
f	heat flux, $[M\theta^{-3}]$ or $[QL^{-2}\theta^{-1}]$
F, F_o	uniform heat flux, $[M\theta^{-3}]$ or $[QL^{-2}\theta^{-1}]$
h	height, [L]
I_i	modified Bessel function of the first kind of order i
J_i	Bessel function of the first kind of order i
k	thermal conductivity, $[ML\theta^{-3}T^{-1}]$ or $[QL^{-1}\theta^{-1}T^{-1}]$
K_i	modified Bessel function of the second kind of order i
q_b	rate of heat transported by blood, defined by Eq. (2.1), $[ML^{-1}\theta^{-3}]$ or $[QL^{-3}\theta^{-1}]$
Q_i	defined by Eq. (2.13), $[L^{-2}T]$
$q_m, \dot{Q}_i$	internal heat generation rate per unit volume, $[ML^{-1}\theta^{-3}]$ or $[QL^{-3}\theta^{-1}]$
Q_m	total metabolic rate, $[ML^2\theta^{-3}]$ or $[Q\theta^{-1}]$
r	radial coordinate, [L]
R_1	radius of inner core in cylindrical model, [L]
R_{12}	radius of interface between skeletal muscle and skin layer in cylindrical model, [L]
R_2	radius of the skin surface in cylindrical model, [L]

†Units in brackets are: M, mass; L, length; θ, time; T, temperature; Q, heat $[ML^2\theta^{-2}]$.

t	time, $[\theta]$
t^*	characteristic time, $[\theta]$
T	tissue temperature, $[T]$
T_a	arterial blood temperature, $[T]$
T_1	constant temperature at inner core, $[T]$
V	volume, $[L^3]$
w_b	blood perfusion rate per unit volume, $[ML^{-3}\theta^{-1}]$
w_i	defined by Eq. (2.12), $[L^{-1}]$
W	weight, $[ML\theta^{-2}]$
Y_i	Bessel function of the second kind of order i
z	coordinate, parallel to the axis of the cylinder, $[L]$
α	thermal diffusivity, $[L^2\theta^{-1}]$
$\alpha_{n,i}$	defined by Eq. (2.17), $[L^{-1}T]$
β	ratio of width of cooling tube to cooling tube spacing
ϵ_i	defined by Eq. (2.22), $[L^{-1}]$
ζ_i	defined by Eq. (2.15), $[L^{-1}]$
η	ratio of heat fluxes of the uncontacted to the contacted skin
θ	defined by Eq. (2.11), $[T]$
λ_n	defined by Eq. (2.16), $[L^{-1}]$
ξ	dummy variable of integration, $[L]$
μ_n	defined by Eq. (2.21), $[L^{-1}]$
ρ	specific density of tissue, $[ML^{-3}]$
σ_n	defined by Eq. (2.20)
ϕ	angular coordinate
χ_n	defined by Eq. (2.19)
$\psi^j_{k\ell}(\zeta_i r)$	combination of modified Bessel functions, defined by Eq. (2.10)

Subscripts

1	pertaining to skin layer or initial state
2	pertaining to skeletal muscle or final state
b	blood
i, j, k, ℓ, n	integer
m	metabolic

LIST OF FIGURES

TABLE OF CONTENTS

1. INTRODUCTION

1.1 BACKGROUND

There are many instances in which it may be desirable to regulate the micro-climate of an individual who is exposed to a thermally hostile environment. One may consider, as examples, the necessity to protect the fire fighter from high temperatures or the need to protect the deep sea diver from low temperatures. Both require some sort of thermal assistance to be able to perform efficiently in their respective environments. In the case of space travel, the astronaut must be protected from a hostile environment for reasons other than strictly thermal ones. Here too, the thermal micro-climate of the astronaut must be controlled in response primarily to his metabolic heat generation rate, a variable which changes with his activity level.

Several attempts have been made at solving the problem of regulating the micro-climate of an individual. One method that has been developed to regulate the thermal micro-climate of the human body is to provide for removal or addition of heat by means of liquid filled cooling or heating tubes in contact with the skin surface. So-called thermal suits have been designed [1]* which consist of individual cooling pads. These cooling pads contact the skin surface of the various major parts of the body, e.g., legs, arms and trunk. Each individual cooling pad consists of tubes held in some geometric pattern.

In general, it is not practical to provide an individual with such a cooling or heating suit if, in doing so, his ability to

*Numbers in brackets refer to entries in REFERENCES.

function efficiently is seriously hindered. Therefore, for most applications, the weight and size of the suit become critical factors. One of the design objectives then would be to minimize the weight and bulk of the suit while maintaining an adequate cooling capacity. When considering the parameters of weight and size as variables governing the efficiency of a man wearing such a suit, weight seems to be most significant. With respect to weight, there will be some optimum combination of cooling tube size and spacing that will provide an adequate cooling or heating capacity.

To date little work has been done on the problem of defining an optimum relationship between cooling capacity, tube size and spacing. A potential contribution to the solution of this problem would be to develop an analytical model of human tissue in contact with a network of cooling tubes. Such a model should facilitate the prediction of heat fluxes and temperature distributions in the tissue. The validity of such a model could be verified by experimental methods.

The purpose of this work was to obtain a solution for such a model [1] and then to compare the calculated results with experimental data.

1.2 REVIEW OF RELATED STUDIES

For the past few decades studies have been conducted dealing with the problem of analytical modeling of the human thermal system and with the measurement of thermophysical properties of human tissue. The results of some comprehensive work done in the area of analytical modeling is presented in a report by Shitzer, Chato and Hertig [1]. In their work, the authors develop the so-called

biothermal model for various geometries.

Some experimental work has been done in an attempt to provide a thermally controllable micro-climate for an individual. The concept of a water cooled suit was first suggested in 1958 by Billingham [2] and a prototype suit was constructed at the Royal Aircraft Establishment in 1964 by Burton and Collier [3]. Their primary interest was protection of crewmembers in hot environments such as sunlit aircraft cockpits, but it was realized that practical personal cooling would have many possible applications. In general, the suit was thought of as a form-fitting heat exchanger in which water absorbed heat from the pilot's body as it passed through tubes over the skin. The heat was then dissipated by an external heat sink. By analogy with the circulation, the process is generally called convective cooling [3] although other investigators refer to it as "conductive cooling" [4,5].

A prototype water cooled garment (WCG) was built [3] of 40 PVC tubes sewn to a suit of cotton underwear. Water was piped to the ankles and wrists where manifolds distributed it to smaller tubes which ran back over the limbs to the outlet manifolds at the mid-thorax. The head and neck were not cooled. Preliminary tests indicated excellent thermal coupling between the skin and water stream [3]. The suit was comfortable even when high heat loads necessitated low water temperatures and despite the existence of wide differences in skin temperatures when comparing sites directly beneath the cooling tubes with sites lying between the tubes [6,7].

Following a demonstration of the British WCG at Houston [3], development of similar garments in the United States was undertaken

for the National Aeronautics and Space Administration (NASA), [8,9]. A series of suits was designed with the distribution of tubing proportional to body mass and with water flow from the extremities toward the torso. Experiments demonstrated the practicality of the WCG as a sole heat sink for men working at metabolic rates up to 2000 Btu/hr, which was the expected activity level rate for lunar surface activity. Cooling virtually eliminated sweating, and for any given work rate subjective comfort included a surprisingly wide envelope of water flow and temperature combinations. Other results showed that heat output rose sharply over working muscle groups, e.g., leg versus arm work [8], and that the interposition of any material between skin and tubing caused significant reduction in cooling efficiency [9].

Direct comparison of air and water cooling in pressure suits showed the latter to be far more effective in reducing signs of heat stress such as sweat rate and rectal temperature rise. Subjective comfort was also much improved by the WCG. These findings applied whether the heat stress was due to a hot environment [10, 11] or high work rates [12,13].

The Apollo water cooled garment is a system of clear plastic tubes sewn inside a suit of stretch underwear with an added nylon slip layer between tubing and skin [4,5,9]. Cooling is provided for the torso and legs but excludes the head and neck. Water flows through 40 tubes in a loop pattern which begins and ends in manifolds located at mid-torso. Flow rate is fixed at 237.6 lb/hr (1.8 liters/min) with manual operation of a diverter valve to

produce water inlet temperatures of 44.1°F (6.7°C), 59.9°F (15.5°C), or 71.6°F (22°C). The external heat sink is located in the back pack where water from a separate supply is sublimated to space. It is designed to handle continuous loads of 1600 Btu/hr (469 w) with peaks to 2000 Btu/hr (586 w). Plans for lunar extra vehicular-activity (EVA) have been tailored to this limit. Lunar surface activities on Apollo 11 and 12 averaged 800 to 1200 Btu/hr (234 to 352 w) [4]. In the case of Apollo 14, actual levels of 2500 Btu/hr (720 w) were attained, exceeding the design limit. The resulting heat storage caused noticeable signs of heat strain and much discomfort [14].

At least one group of researchers [7] has considered the problem of an optimum relationship between cooling tube size and spacing. In this study experiments were performed in which the tube spacing was considered as the only variable. The experimental work indicated that the temperature differences on the skin were of the order of 8°F (4.45°C) with 1-in. spacing of 1/8-in. O.D. cooling tubes and 3.5°F (1.94°C) with 0.5-in. spacing of the same tubes. The temperature profile on the skin was found to develop approximately three times as fast with the closer spacing.

1.3 SPECIFIC STATEMENT OF THE PROBLEM

Consideration of the biothermal model of human tissue in contact with a network of parallel cooling tubes [1] led to the following three basic objectives of this study:

1. To obtain the solution of the biothermal model for the steady state and transient cases in cylindrical coordinates.
2. To construct three different cooling pads and to perform experiments with them. It is hoped that the results may be

used to gain some insight into the validity of the biothermal model and its solution, and

3. To compare experimental data for the three cooling pads, each pad having a different combination of cooling tube size and spacing.

The solution of the biothermal model should predict the temperature profile on the skin surface between adjacent cooling tubes. The objective of the experimental scheme, then, was to construct a cooling pad and to measure the temperature distribution between the tubes corresponding to various activity levels. Three different cooling pad configurations were tested. The corresponding measured results were then compared to each other and related to the analytical predictions.

1.4 SCOPE OF THE STUDY AND LIMITATIONS

Experimental measurement of the temperature distribution between cooling tubes were limited to data taken on the skin surface of the human thigh. Measurements were taken for three different cooling pads at four metabolic activity levels. In general, the four activity categories and associated metabolic rates were:

1. Standing, 300 Btu/hr (88 w);
2. Mild work, 600 Btu/hr (176 w);
3. Moderate work, 900 Btu/hr (264 w); and
4. Heavy work, 1800 Btu/hr (528 w).

The metabolic levels associated with mild, moderate and heavy work were attained by the subject as he rode on a variable load bicycle ergometer. During the individual experiments the transient temperature

distribution was also measured as the subject's metabolic rate changed from one level to another.

Since the experimental measurements of the temperature distribution was limited to the thigh only, the solution to the biothermal model was obtained in cylindrical coordinates. Engineering judgment, as applied to thermal systems, suggested the modeling of the leg as a cylinder of finite length. There were, however, a number of assumptions and limitations to be considered when modeling the human body. The thermophysical properties of human tissue and their detailed relationship to the formulation of the analytical model will be discussed later.

2. THEORETICAL ANALYSIS

2.1 THE BIOTHERMAL MODEL WITH DEVELOPMENT OF THE GOVERNING PARTIAL DIFFERENTIAL EQUATION

The problem of developing an analytical expression to describe the thermal behavior of living human tissue is indeed very complex. At this time, even the most basic of the mechanisms that govern heat transfer in living tissue remain unexplained, i.e., the exact nature of blood perfusion and metabolic heat generation rates have yet to be described and measured in detail. The problem is further complicated by the lack of accurate data on the thermophysical properties of living tissue. Thus, several assumptions had to be made before an analytical model could be developed.

1. The thermophysical properties of the tissue were assumed to be constant in time and space and the tissue to be homogeneous and isotropic.
2. The temperature of the blood leaving the tissue was assumed to equal the temperature of the tissue.
3. The temperature of the blood flowing into the tissue was assumed constant and equal to the temperature of the artery.
4. Blood perfusion rates and metabolic heat generation rates were assumed uniform and constant throughout the entire layer of tissue [15].

The values associated with these rates were considered as average values.

The storage, conduction and production of heat within the tissue could be represented by well known expressions in heat transfer. An additional term was needed to represent the heat

transported by the blood stream. It was assumed that the amount of heat gained by the tissue due to blood perfusion was [1]

$$q_b = w_b c_b (T_a - T) \tag{2.1}$$

Equation (2.1), when substituted into the heat equation, yields the general form which describes the biothermal model:

$$\rho c_p \frac{\partial T}{\partial t} = k\nabla^2 T + w_b c_b (T_a - T) + q_m \tag{2.2}$$

Equation (2.2) is a mathematical statement of the first law of thermodynamics describing the "in vivo" relationship between the various modes of heat transfer, storage, and production within biological tissue. It was referred to as the "bio-heat" equation [1]. Similar forms have been obtained by Pennes [16], Hertzman [17], Wissler [18], Perl [19], Chato [20], Trezek [21] and Keller and Seiler [22].

2.2 GEOMETRY, BOUNDARY AND INITIAL CONDITIONS

2.2.1 Geometry

The experimental phase of this study was concerned with the removal of metabolic heat produced in the thigh muscles as the human subject engaged in various levels of activity. The experimental cooling pads have been designed such that the cooling tubes were in direct contact with the skin surface. The cooling pad was placed around the thigh with the axis of the tubes perpendicular to the axis of the leg, as illustrated in Fig. 2.1. Consequently, the geometry of the thigh was approximated by a circular cylinder.

The living tissue that composes the thigh can be divided into

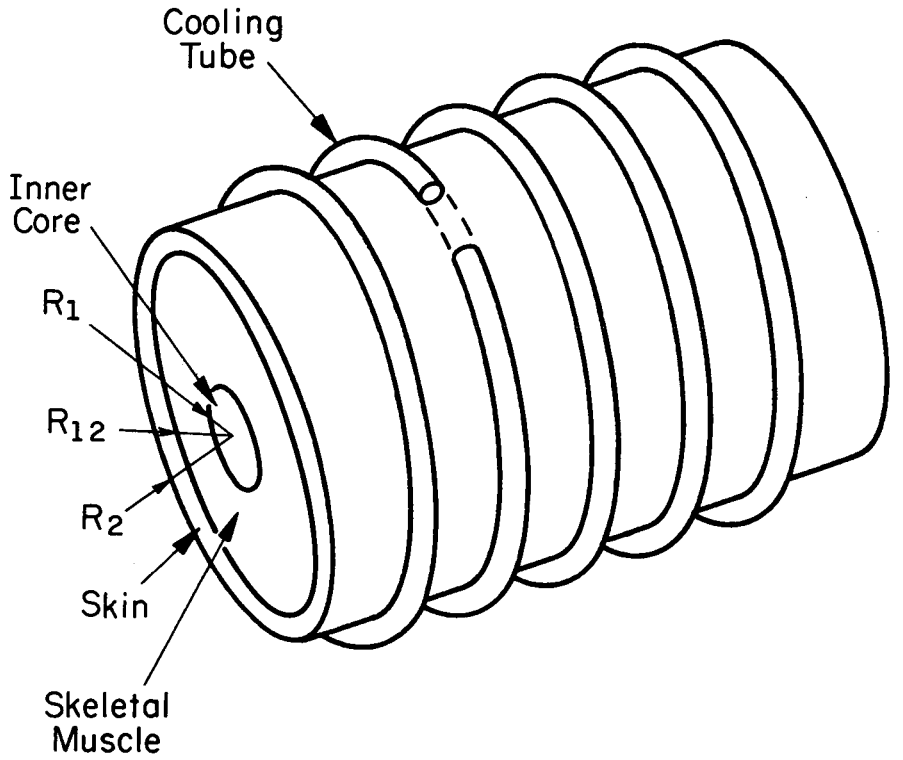

Figure 2.1 Representative section of the cylindrical model with the cooling tubes on the skin running perpendicular to the axis of the cylinder.

three layers:

1. A skin layer composed of epidermis, dermis, and subcutaneous fat. The total thickness of these layers varies from 1 to 6 mm [23]. In the model all excess metabolic heat was assumed to be removed at the contact areas between the epidermis and cooling tubes,
2. A layer of skeletal muscle, and
3. An inner core layer consisting of bone and all the internal members. At steady state this layer was assumed to be at a constant temperature.

For steady state conditions the first two layers were treated separately [1], but for the transient cases it was assumed that these layers could be approximated by a single, combined layer with averaged properties.

2.2.2 Boundary and Initial Conditions

The temperature of the interface between the skeletal muscle and the inner core was assumed constant and uniform and equal to that of the inner core. At the skin surface, a heat flux corresponding to the amount of heat removed by the cooling tubes was assumed. No heat was considered to be removed from the remaining areas of the skin which were not in contact with the cooling tubes. A representation of the leg as a cylinder covered with equally spaced cooling tubes running perpendicular to the axis of the cylinder, Fig. 2.1, rendered the problem geometrically symmetrical. Consequently, the lines of symmetry running through the tubes and one-half the distance between the two adjacent tubes could be considered as adiabatic planes.

Gradients along the cooling tubes were assumed to be negligibly

small when compared to those occurring in a direction perpendicular to the tubes. In mathematical terms

$$\frac{\partial}{\partial \phi} = 0 \tag{2.3}$$

and the problem becomes two-dimensional in r and z.

The steady state temperature distribution in the tissue at a given metabolic rate was assumed to be the initial condition for the transient state. The geometry and associated boundary conditions for this problem are shown in Fig. 2.2. In the analysis presented below, the skin and skeletal muscle were considered to constitute a combined region. The problem as formulated then becomes

$$\frac{1}{\alpha}\frac{\partial \theta}{\partial t} = \frac{1}{r}\frac{\partial}{\partial r}\left(r\frac{\partial \theta}{\partial r}\right) + \frac{\partial^2 \theta}{\partial z^2} - w_2^2\theta + Q_2 \tag{2.4}$$

such that

$$R_1 \leq r \leq R_2, \quad 0 \leq z \leq a \; ; \quad t \geq 0$$

with the boundary and initial conditions:

at

$$r = R_1 \; , \quad \theta = 0 \tag{2.5}$$

at

$$r = R_2 \; , \left\{ \begin{array}{ll} \dfrac{\partial \theta}{\partial r} = \dfrac{f_2(z)}{k} \; , & 0 \leq z < \beta a \\ \dfrac{\partial \theta}{\partial r} = 0 \; , & \beta a < z \leq a \end{array} \right\} \tag{2.6}$$

at

$$z = 0 \; , \quad \frac{\partial \theta}{\partial z} = 0 \tag{2.7}$$

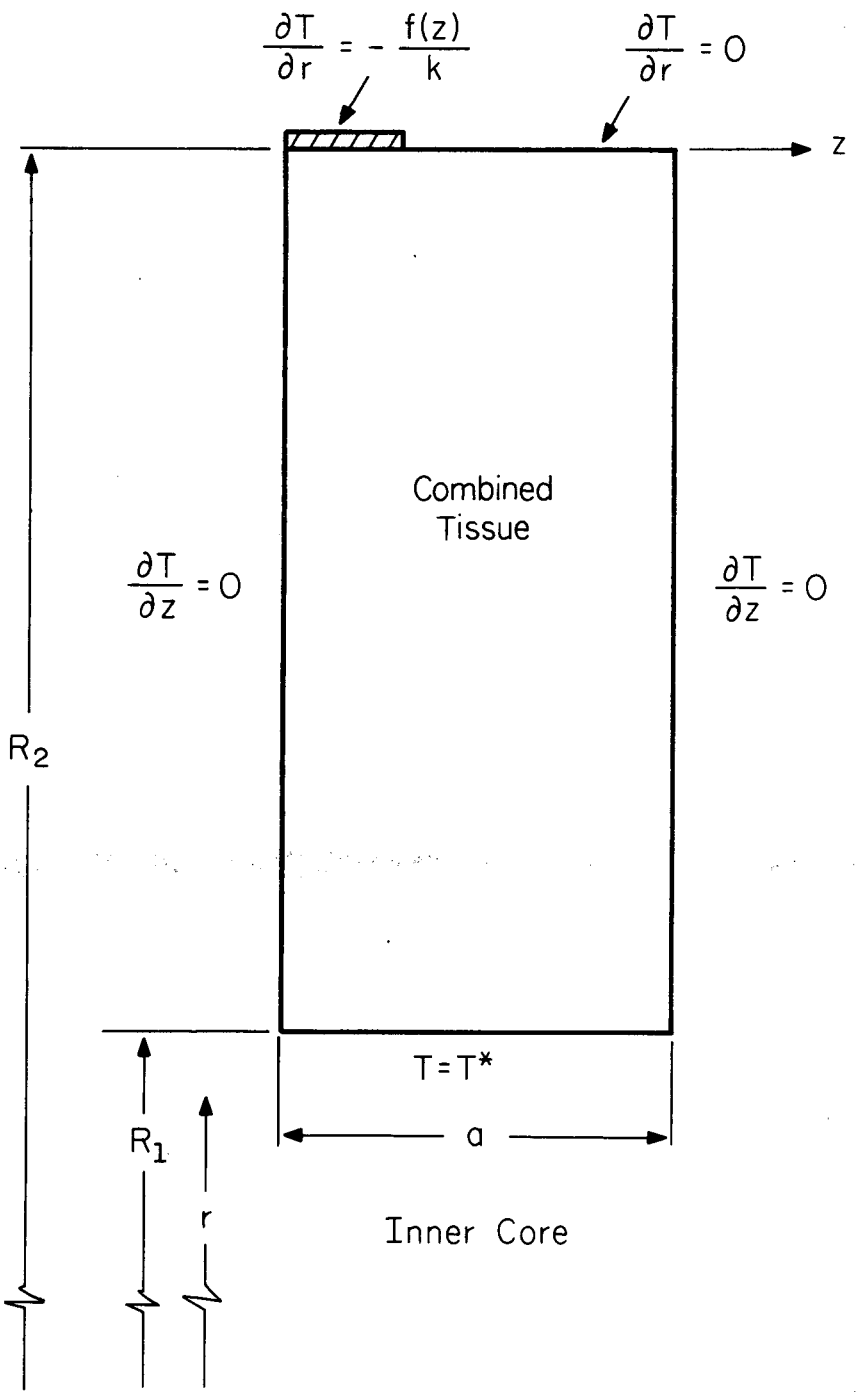

Figure 2.2 Geometry and boundary conditions for the cylindrical model with the cooling tubes on the skin running perpendicular to the axis of the cylinder. Skin layer and skeletal muscle are considered as a combined region.

at

$$z = a \ , \quad \frac{\partial \theta}{\partial z} = 0 \tag{2.8}$$

at

$$t < 0 \ , \quad \theta = \frac{Q_1}{w_1^2}\left[1 - \frac{\psi_{01}^2(w_1 r)}{\psi_{01}^2(w_1 R_1)}\right] - \frac{\beta f_{a,1}}{k w_1}\frac{\psi_{00}^1(w_1 r)}{\psi_{01}^2(w_1 R_1)} - \sum_{n=1}^{\infty} \frac{\alpha_{n,1}\psi_{00}^1(\zeta_1 r)}{\zeta_1 \psi_{01}^2(\zeta_1 R_1)} \cos(\lambda_n z) \tag{2.9}$$

where

$$\psi_{k\ell}^j(\zeta_i r) \equiv I_k(\zeta_i r)\, K_\ell(\zeta_i R_j) - (-1)^{k+\ell} I_\ell(\zeta_i R_j)\, K_k(\zeta_i r) \tag{2.10}$$

I_i and K_i are the modified Bessel functions of the first and second kind, respectively, of order i. The other parameters appearing in Eq. (2.9) are defined by

$$\theta = T(r,z) - T_1 \tag{2.11}$$

$$w_i^2 = \frac{w_{b,i} c_b}{k} \tag{2.12}$$

$$Q_i = \frac{\dot{Q}_i + w_{b,i} c_b (T_a - T_1)}{k} \tag{2.13}$$

$$f_{a,i} = \frac{1}{\beta a}\int_0^{\beta a} f_i(\xi)\, d\xi \tag{2.14}$$

$$\zeta_i^2 = w_i^2 + \lambda_n^2 \tag{2.15}$$

$$\lambda_n \equiv \frac{n\pi}{a} \tag{2.16}$$

$$\alpha_{n,i} = \frac{2}{a} \int_0^{\beta a} \frac{f_i(\xi)}{k} \cos(\lambda_n \xi)\, d\xi \qquad (2.17)$$

The special function $\psi^j_{k\ell}(\zeta_i r)$ was defined to simplify the mathematical derivation of Eq. (2.9) [1]. It is a combination of modified Bessel functions of the first and second kinds which was found to recur in the solution many times.

Solution to the above set of equations and boundary and initial conditions was obtained by employing the technique of separating the variables to yield

$$\begin{aligned} T(r,z,t) = T_1 &+ \frac{Q_2}{w_2^2}\left[1 - \frac{\psi^2_{01}(w_2 r)}{\psi^2_{01}(w_2 R_1)}\right] - \frac{\beta f_{a,2}}{k w_2} \frac{\psi^1_{00}(w_2 r)}{\psi^2_{01}(w_2 R_1)} \\ &- \sum_{n=1}^{\infty} \frac{\alpha_{n,2}\psi^1_{00}(\zeta_2 r)}{\zeta_2 \psi^2_{01}(\zeta_2 R_1)} \cos(\lambda_n z) \\ &+ \frac{2\pi}{k} \sum_{n=1}^{\infty} \frac{2\left[\frac{\dot{Q}_2}{\varepsilon_2^2} - \frac{\dot{Q}_1}{\varepsilon_1^2}\right] + \beta\mu_n \sigma_n(\mu_n R_2)\left[\frac{f_{a,2}}{\varepsilon_2^2} - \frac{f_{a,1}}{\varepsilon_1^2}\right]}{\sigma_n^2(\mu_n R_2) - 4} \\ &\cdot \chi_n(\mu_n r) \exp[-\alpha\varepsilon_2^2 t] \\ &+ 2\pi \sum_{m=1}^{\infty}\sum_{n=1}^{\infty} \left[\frac{\alpha_{m,2}}{\varepsilon_2^2 + \lambda_m^2} - \frac{\alpha_{m,1}}{\varepsilon_1^2 + \lambda_m^2}\right] \frac{\mu_n \sigma_n(\mu_n R_2)}{\sigma_n^2(\mu_n R_2) - 4} \\ &\cdot \chi_n(\mu_n r) \cos(\lambda_m z) \exp\{-\alpha[\varepsilon_2^2 + \lambda_m^2]t\} \end{aligned} \qquad (2.18)$$

where

$$\chi_n(\mu_n r) = J_o(\mu_n r)Y_o(\mu_n R_1) - J_o(\mu_n R_1)Y_o(\mu_n r) \quad (2.19)$$

J_o and Y_o are the Bessel functions of the first and second kind, respectively, of order zero.

$$\sigma_n(\mu_n R_2) = \pi(\mu_n R_2)\chi_n(\mu_n R_2) \quad (2.20)$$

μ_n's are the roots of

$$J_o(\mu_n R_1)Y_1(\mu_n R_2) - J_1(\mu_n R_2)Y_o(\mu_n R_1) = 0 \quad (2.21)$$

and

$$\epsilon_i^2 = \mu_n^2 + w_i^2 \quad (2.22)$$

The first fifteen eigenvalues, μ_n, were computed using Newton-Raphson's method. Results are present in TABLE 2.1. As the ratio R_2/R_1 approaches unity (rectangular model), or as n increases, the eigenvalues approach those of the rectangular model, $\mu_n \rightarrow [(2n - 1)\pi]/2b$, as is to be expected.

Numerical values of transient temperature distributions in the tissue and on the skin surface were obtained with the aid of a digital computer.

Figures 2.3 and 2.4 show results obtained for a one-dimensional model (uniform cooling of the skin). Step changes in activity level were assumed from low (290 Btu/hr, 85 w) to high (2600 Btu/hr, 760 w) and reversed, respectively. The substantial changes in the

TABLE 2.1

FIRST 15 ROOTS OF EQ. (2.21) AS A FUNCTION OF THE RATIO OF THE OUTER TO INNER RADII OF THE CYLINDRICAL MODEL, R_2/R_1. THE RIGHTMOST COLUMN GIVES THE ASYMPTOTIC VALUES, $[(2n - 1)\pi/2b]$, AS $R_1 \to \infty$ AND $R_2/R_1 \to 1$ (RECTANGULAR MODEL)

R_2/R_1	2.46	1.73	1.37	1.24	1.19	1.15	1.00
R_1 (ft)	0.05	0.10	0.20	0.30	0.40	0.50	$\to\infty$
n							
1	17.827850	19.184982	20.156525	20.550354	20.764221	20.898514	21.48830
2	63.293686	63.736526	64.037781	64.161377	64.229202	64.272369	64.46491
3	106.737122	107.005951	107.186890	107.258667	107.301025	107.326599	107.44152
4	149.914780	150.107346	150.236740	150.285004	150.316589	150.336288	150.41813
5	193.003647	193.153290	193.244324	193.295212	193.316849	193.331406	193.39473
6	236.050980	236.173935	236.252670	236.290054	236.304901	236.319809	236.37134
7	279.075439	279.179932	279.249756	279.279053	279.293457	279.304688	279.34795
8	322.091553	322.179932	322.240234	322.263428	322.278320	322.287598	322.32455
9	365.093994	365.173584	365.227051	365.244385	365.258789	365.268799	365.30116
10	408.092285	408.152588	408.201416	408.232178	408.241211	408.249512	408.27777
11	451.093018	451.151367	451.190430	451.213135	451.250000	451.229492	451.25438
12	494.078369	494.135498	494.175537	494.193115	494.200439	494.210205	494.23098
13	537.066895	537.121094	537.157959	537.171143	537.180664	537.189453	537.20759
14	580.054199	580.104248	580.114258	580.147217	580.156982	580.167480	580.18420
15	623.040283	623.073730	623.105957	623.132324	623.138916	623.145508	623.16080

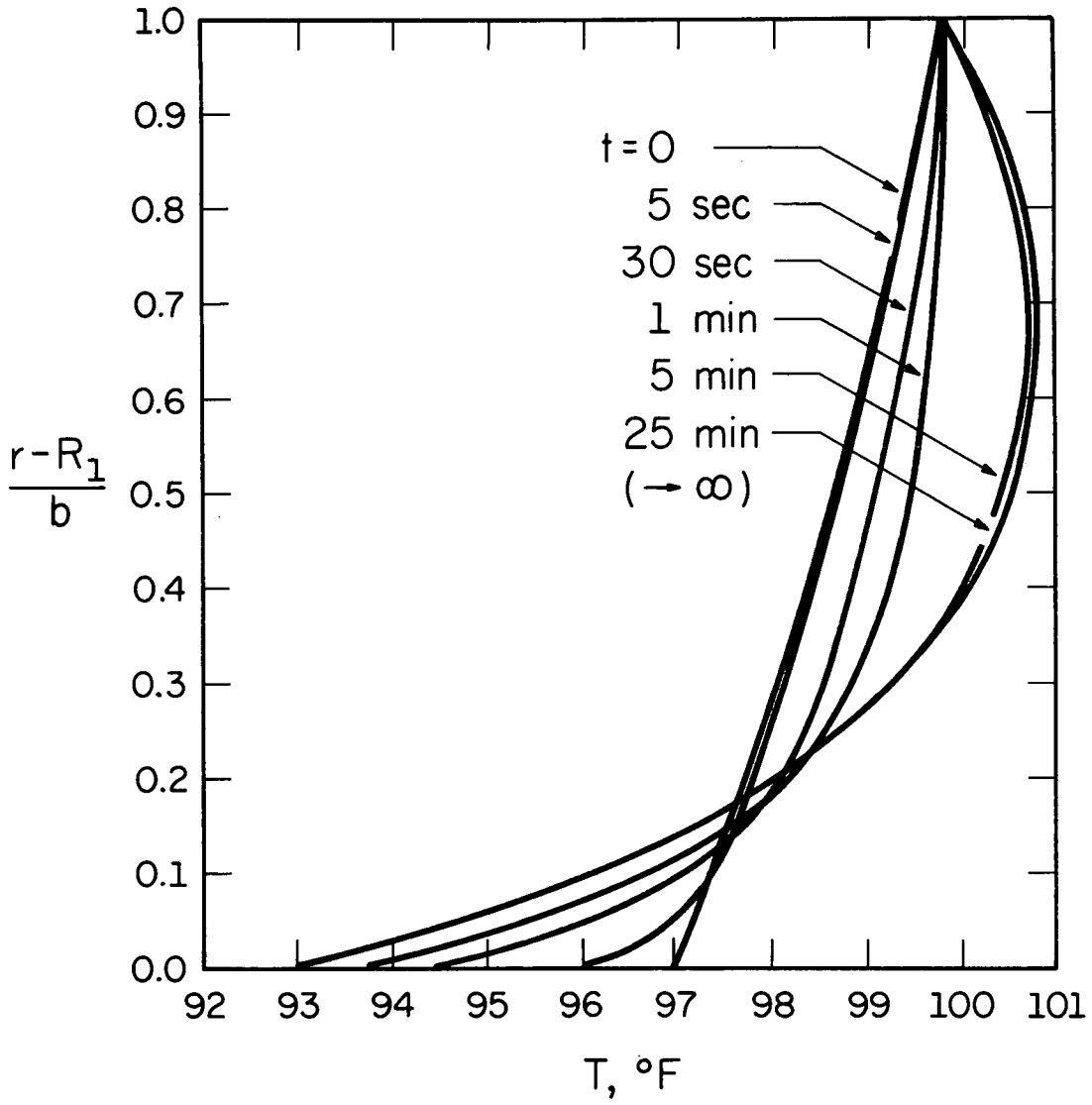

Figure 2.3 Temperature distributions in the tissue for the one-dimensional, cylindrical model. Step change is from low (290 Btu/hr, 85 w) to high (2600 Btu/hr, 760 w) activity level. Constant temperature of 99.7°F (37.7°C) at the inner core, R_1 = 0.15 ft (4.6 cm), A and b are constant.

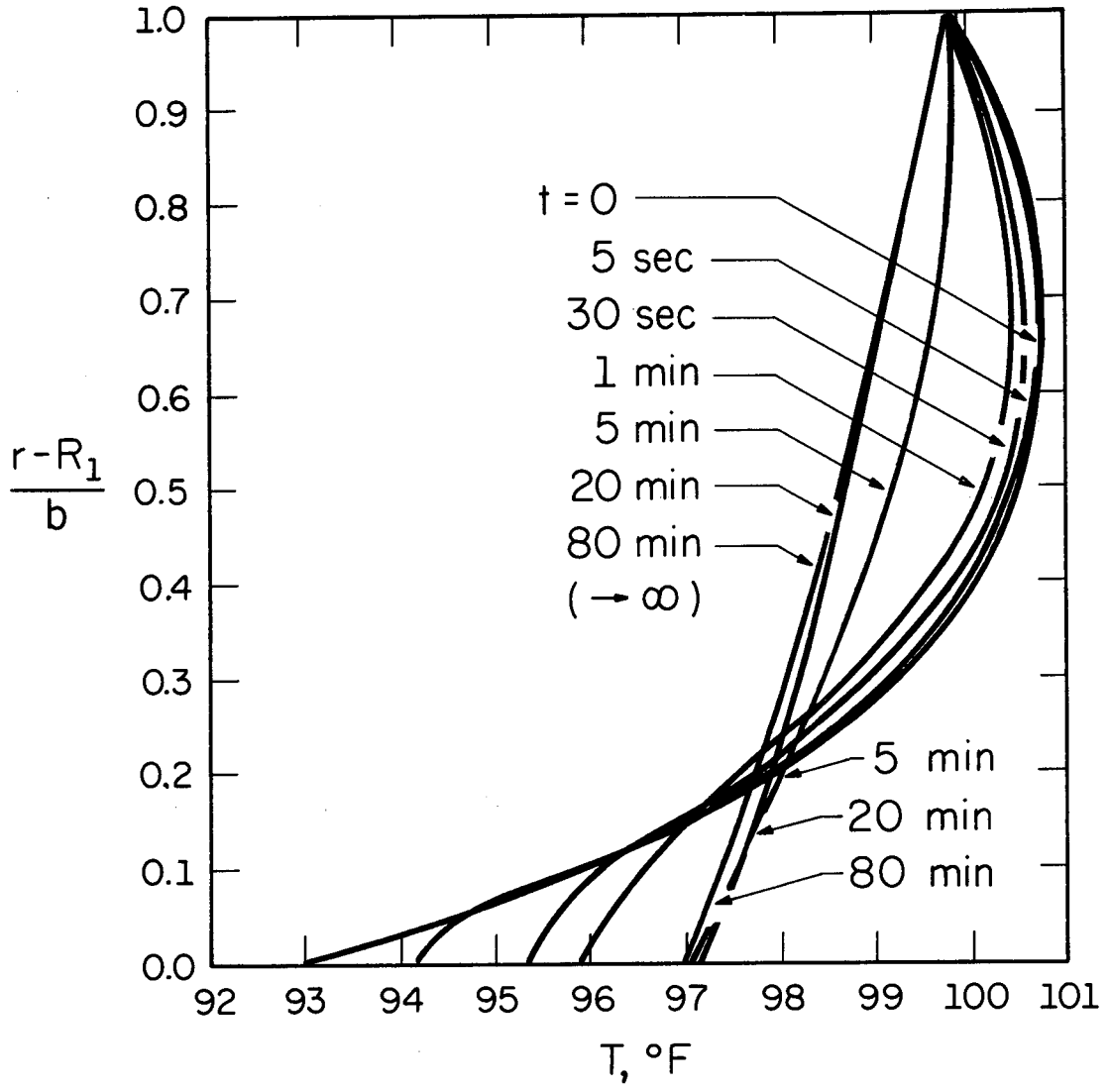

Figure 2.4 Temperature distributions in the tissue for the one-dimensional, cylindrical model. Step change is from high (2600 Btu/hr, 760 w) to low (290 Btu/hr, 85 w) activity level. Constant temperature of 99.7°F (37.7°C) at the inner core, R_1 = 0.15 ft (4.6 cm), A and b are constant.

temperature of the tissue were found to occur during the first 5 minutes from the onset of the change from low to high activity level. When the change is reversed, substantial temperature variations occur during the first 25 minutes, approximately. The final steady state temperature profile is attained after 25 (low to high) and 80 (high to low) minutes. The ratio of these time constants was supported by the experimental results.

In Fig. 2.5 temperature variations on the skin of the cylindrical model are shown. Time constants associated with this two-dimensional geometry were found to be identical to those obtained for one-dimensional configurations [1].

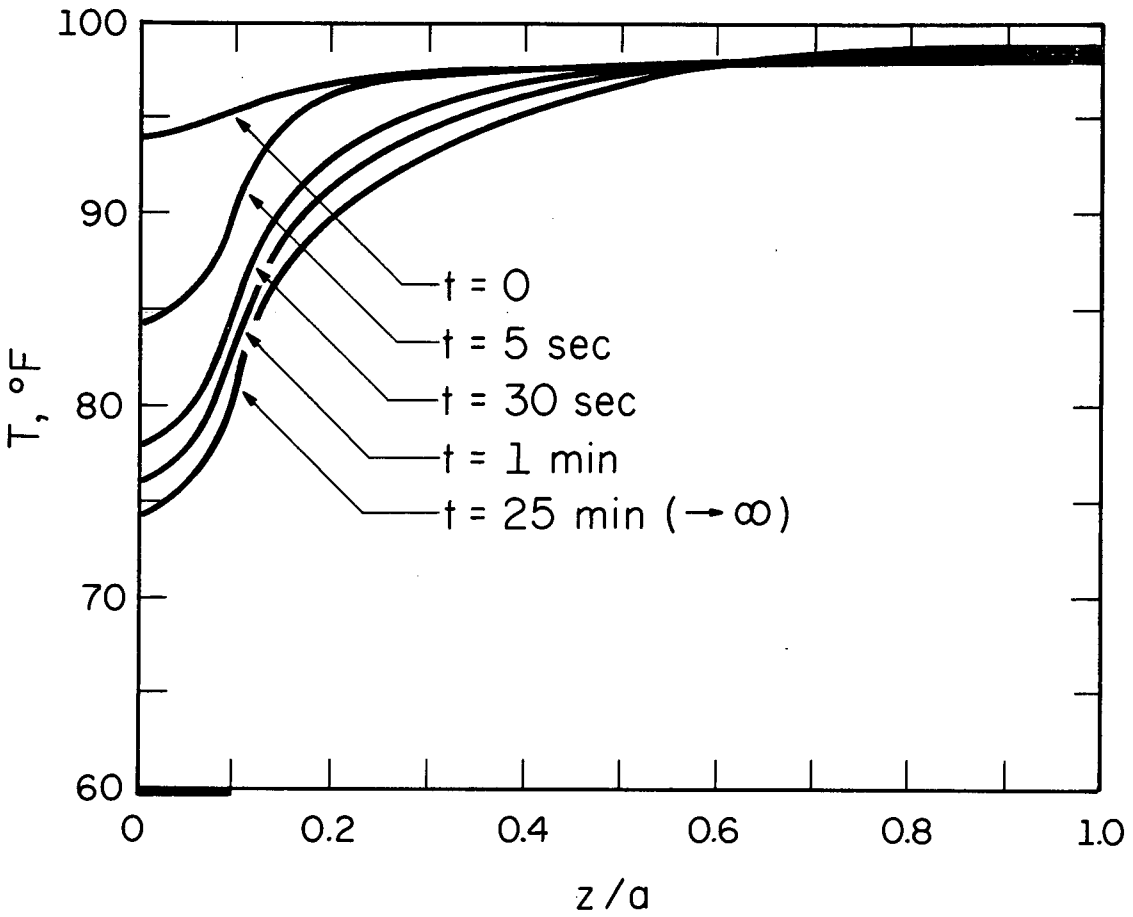

Figure 2.5 Temperature distributions on the skin surface for the two-dimensional, cylindrical model. Step change is from low (290 Btu/hr, 85 w) to high (2600 Btu/hr, 760 w) activity level. $\beta = 0.1$, constant temperature of 99.7°F, (37.7°C) at the inner core, $R_1 = 0.15$ ft (4.6 cm), A and b are constant.

3. EXPERIMENTS

3.1 OBJECTIVES

The basic objective of the experimental phase of the study was to measure the temperature distribution on the skin surface between adjacent tubes of cooling pads placed around a human thigh. This temperature distribution was measured during activity levels corresponding to low, mild, moderate and high metabolic rates. Also, the temperature distribution was monitored during the transient periods between those activity levels. A secondary objective was to evaluate the effect that various cooling tube sizes and spacings have on the temperature distribution and the overall cooling efficiency. Three cooling pads with different tube size and spacing were tested on a human subject while performing various experimental activity schedules. Figure 3.1 is a schematic diagram of the experimental setup showing the water supply, cooling pad and temperature measuring equipment.

3.2 EXPERIMENTAL APPARATUS

3.2.1 The Individual Pads

Three different cooling pads were built and tested. These pads were specifically designed to fit over the right thigh of the test subject. All three pads were constructed of a flexible, elastic sheet of 1/8-in. gum rubber. Tygon tubes were affixed in a parallel configuration to one side of the pads using Eastman Kodak 910 adhesive. The diameter and spacing of tubes were constant for each individual pad, but varied from pad to pad. TABLE 3.1 gives the pertinent data on the individual pads. Figure 3.2 shows a view

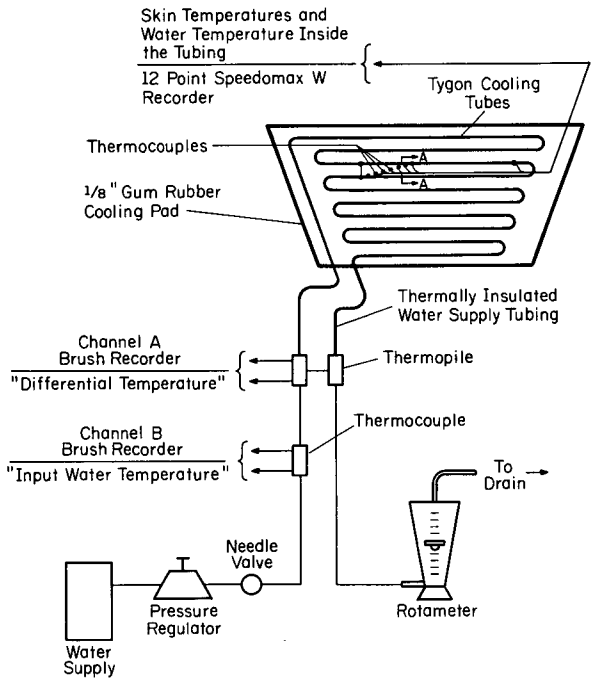

Figure 3.1(a) Schematic diagram of cooling pad and water supply system with temperature measuring points indicated.

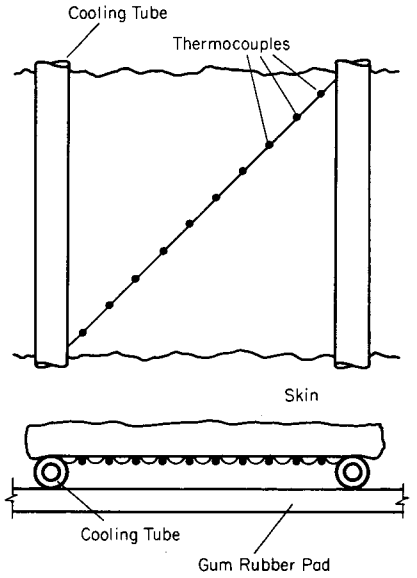

Figure 3.1(b) Cross section A-A showing details of thermocouple placement.

TABLE 3.1

Data On the Individual Cooling Pads

	Outside Diameter of Tubes		Spacing of Tubes		Number of Rows of Tubes	Total Length of Tubes		Area Covered by Pad		Approximate Contact Area with the Skin		Percent of Area in Contact with Tubes
	in.	cm	in.	cm		in.	cm	$in.^2$	cm^2	$in.^2$	cm^2	
Pad No. 1	5/32	0.397	1	2.54	10	163	414	140	910	22.9	148	16.4
Pad No. 2	5/32	0.397	5/8	1.59	14	228	580	132	852	32.1	207	24.3
Pad No. 3	7/32	0.556	1	2.54	10	163	414	145	937	28.5	184	19.7

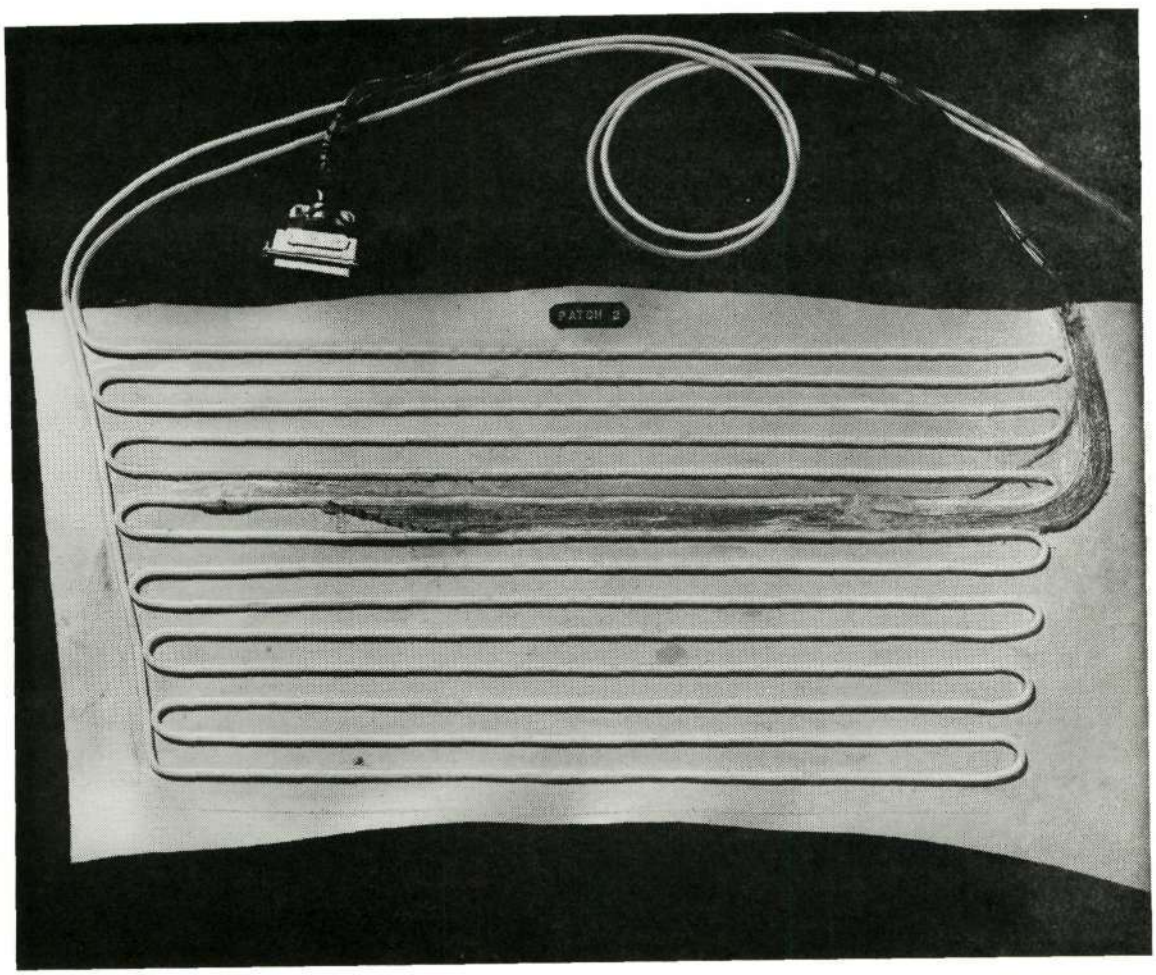

Figure 3.2 View of one of the individual pads.

of one of the individual cooling pads.

Number 30-gauge copper-constantan thermocouples were used to measure cooling water temperatures and skin temperatures between the two adjacent tubes. The thermocouples were equally spaced on a 30 degree diagonal between adjacent cooling tubes. The thermocouples were also located such that they were pressed against the skin surface to insure good thermal contact when the pad was fastened to the thigh. Figure 3.2 illustrates one of the cooling pads and thermocouples.

A Leeds and Northrup Speedomax W, 12-point potentiometer-recorder was used for continuous monitoring and recording of the temperature of the cooling water and the skin temperatures between adjacent tubes. The water supply temperature and the difference between the water outlet and inlet temperatures were continuously recorded by a Brush Mark 280 recorder. Thermopiles consisting of five copper-constantan thermocouples connected in series and a Brush pre-amplifier were used to increase the sensitivity of the reading of the differential water temperature for the pad. The water supply lines leading to the pad were thermally insulated with rubber tubing which provided an air-gap type of thermal barrier.

3.2.2 The Water Supply

The source for the water supply was the cold water line in the laboratory. Before each experiment the cold water was run continuously until an equilibrium temperature was reached and the inlet water temperature became constant at 54.5°F (12.5°C). Figure 3.1 shows the water supply system along with the instrumentation used to record

the experimental data.

The flow rate was maintained constant by a pressure regulator and controlled by a needle valve. The flow rate was measured by a Fischer and Porter Rotameter. All flow rates were maintained constant at 40.5 lb/hr (18.4 kg/hr).

3.2.3 The Metabolic Measurements

For metabolic measurements, expired air samples were taken with a collecting apparatus and stored in metalized Douglas bags [24]. These bags were placed inside a sealed Plexiglas chamber whose pressure was maintained at -5 mm Hg. [25]. Air was inhaled and exhaled through a mouth piece while the nostrils were blocked with a noseclip. Two sets of one-way rubber flap valves insured separation of the two streams. The expired air was directed through a 1-in. I.D. rubber hose into a mixing chamber. One minute sampling was achieved by opening a one-way stopcock valve thus exposing a previously evacuated metalized bag to the exhaled air. The vacuum in the Plexiglas chamber facilitated the filling of the Douglas bags as positive exhaled air pressure existed at the inlet to the bag, and negative chamber pressure surrounded the bag structure.

Air volumetric flow rates were measured by means of a Parkinson-Cowan dry gas meter. Inlet and outlet air temperatures were measured by a Yellow Springs Instrument, Co. Tele-Thermometer and two No. 401 interchangeable, multipurpose thermistors. Figure 3.3 shows the system used to collect air samples.

Once collected in the individual Douglas bags, the air samples were analyzed for CO_2 and O_2 content. A Godart-Mijnhardt CO_2 thermal-

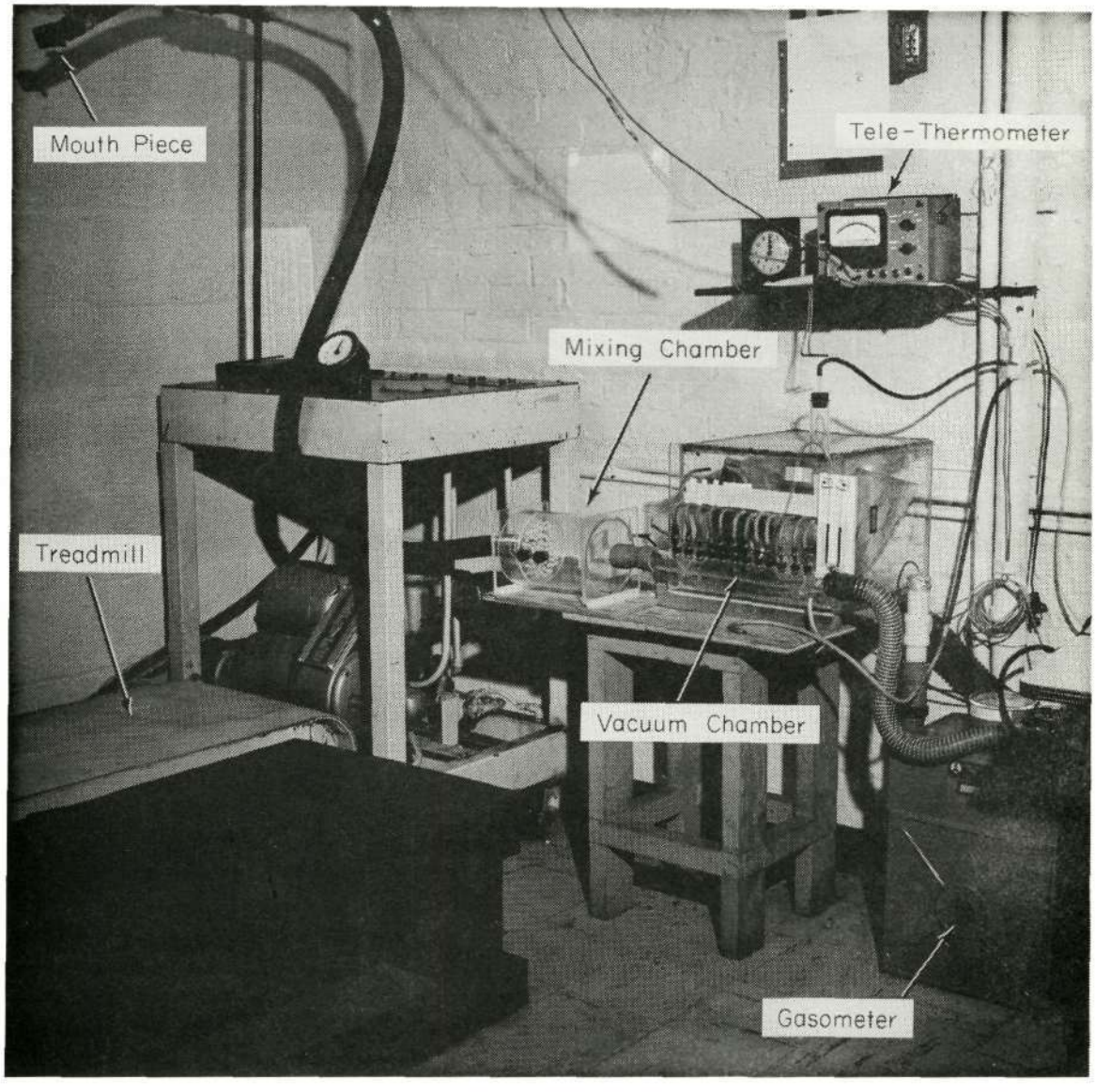

Figure 3.3 A view of the Tele-Thermometer and system for collecting samples for determining metabolic rates.

conductivity meter, Pulmo Analysor Type 44-A-2 and a Beckman Paramagnetic O_2 analyzer, Model C2 were used. The results of this analysis were combined with other data to calculate the metabolic heat generation rate of the subject [26] which is a measure of the energy expenditure. Various levels of energy expenditure were obtained by the subject pedalling a Monark bicycle ergometer at a constant preset speed and load.

3.3 EXPERIMENTAL PROCEDURE AND TEST SCHEDULES

At the beginning of each experiment the ambient temperature, pressure and humidity were recorded. The test subject was weighed and his blood pressure and oral temperature were recorded. During the experiments the test subject wore a sweat shirt, track shorts and tennis shoes. The ear canal temperature was continuously monitored and recorded throughout the duration of the experiment. At the end of the experiment the subject's weight, blood pressure and oral temperature were again measured and recorded.

Figure 3.4 shows the work programs for the experiments. In experiments 1, 2, and 3 the temperature distribution on the skin surface was measured using pad No. 2. Temperature distributions were recorded for these experiments corresponding to activity levels of sitting, standing and mild work, respectively.

Experiments 4, 5, and 6 were conducted using pads No. 1, 2, and 3, respectively. In these experiments the steady state temperature distribution was recorded for a moderate work activity level of 900 Btu/hr (264 w). In experiments 4, 5, and 6 the work load, inlet water temperature and flow rate were maintained at an equal

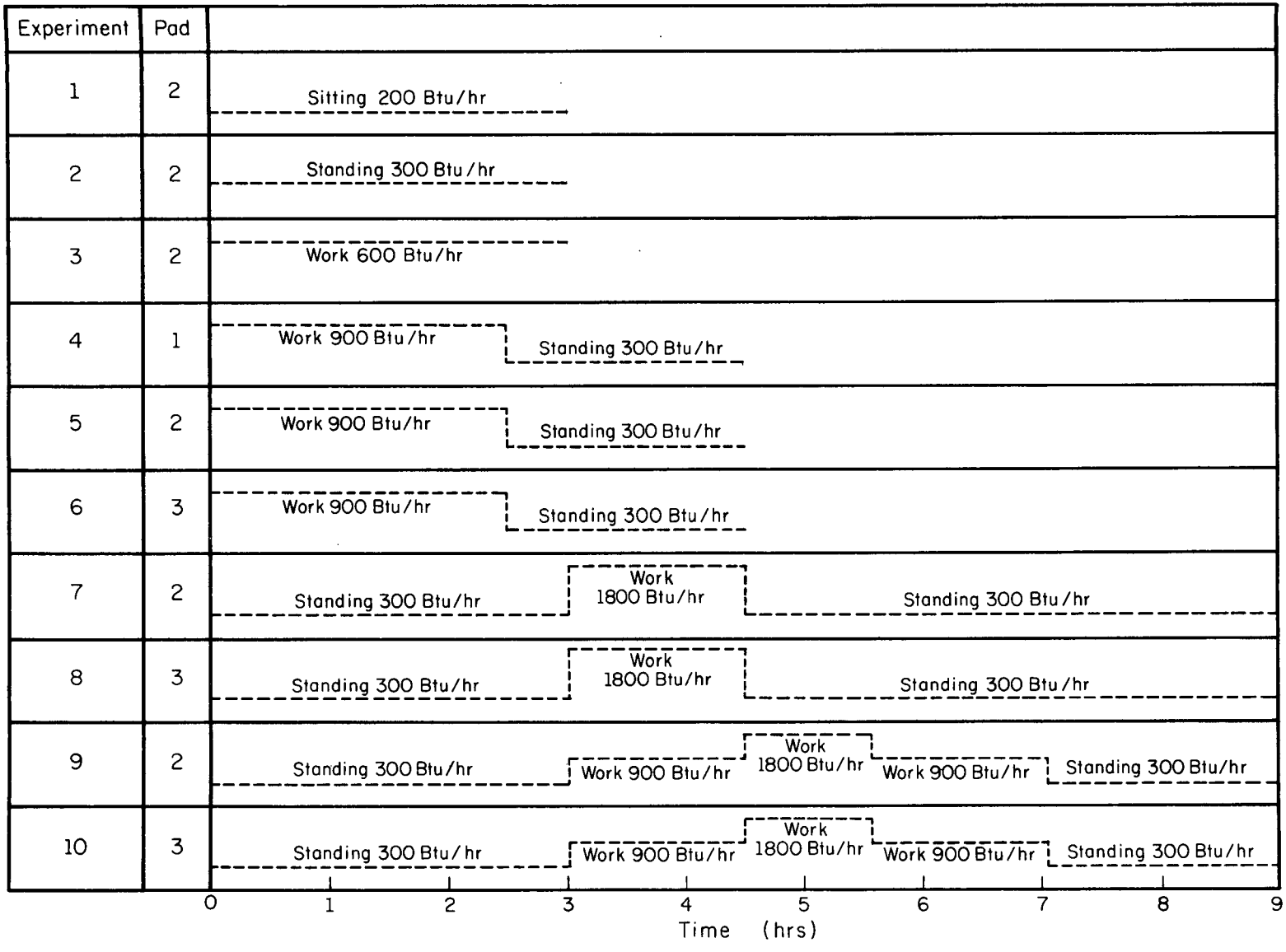

Figure 3.4 Work program for each experiment.

level and held constant for each experiment.

In experiments 7 and 8, cooling pads No. 2 and 3 were used to measure the course of change of the skin temperature distribution resulting from a change in activity level. The temperature distribution was recorded for a change from a steady state level at 300 Btu/hr (88 w) to an elevated level at 1800 Btu/hr (528 w). The change in activity levels during experiments 8, 9 and 10 was achieved by varying the load on the bicyle ergometer. Figure 3.5 shows the test subject pedaling the bicycle ergometer. The test subject continued work at the 1800 Btu/hr (528 w) level until a steady state skin temperature was achieved. At this point the subject stopped working and the resulting transient temperature profile was monitored as he returned to the 300 Btu/hr (88 w) level.

Experiments 9 and 10 were also run with pads No. 2 and 3. Here a similar approach was taken: The temperature distribution was monitored for changes from 300 Btu/hr (88 w) to 900 Btu/hr (264 w) and from 900 Btu/hr (264 w) to 1800 Btu/hr (528 w). The skin temperature profile was recorded again as the test subject decreased activity from 1800 to 900 Btu/hr and finally from 900 to 300 Btu/hr (528, 264, and 88 w, respectively).

3.4 THE TEST SUBJECT

The test subject was a caucasian male student of the University of Illinois at Urbana-Champaign. The subject was in excellent physical condition. TABLE 3.2 illustrates his personal characteristics.

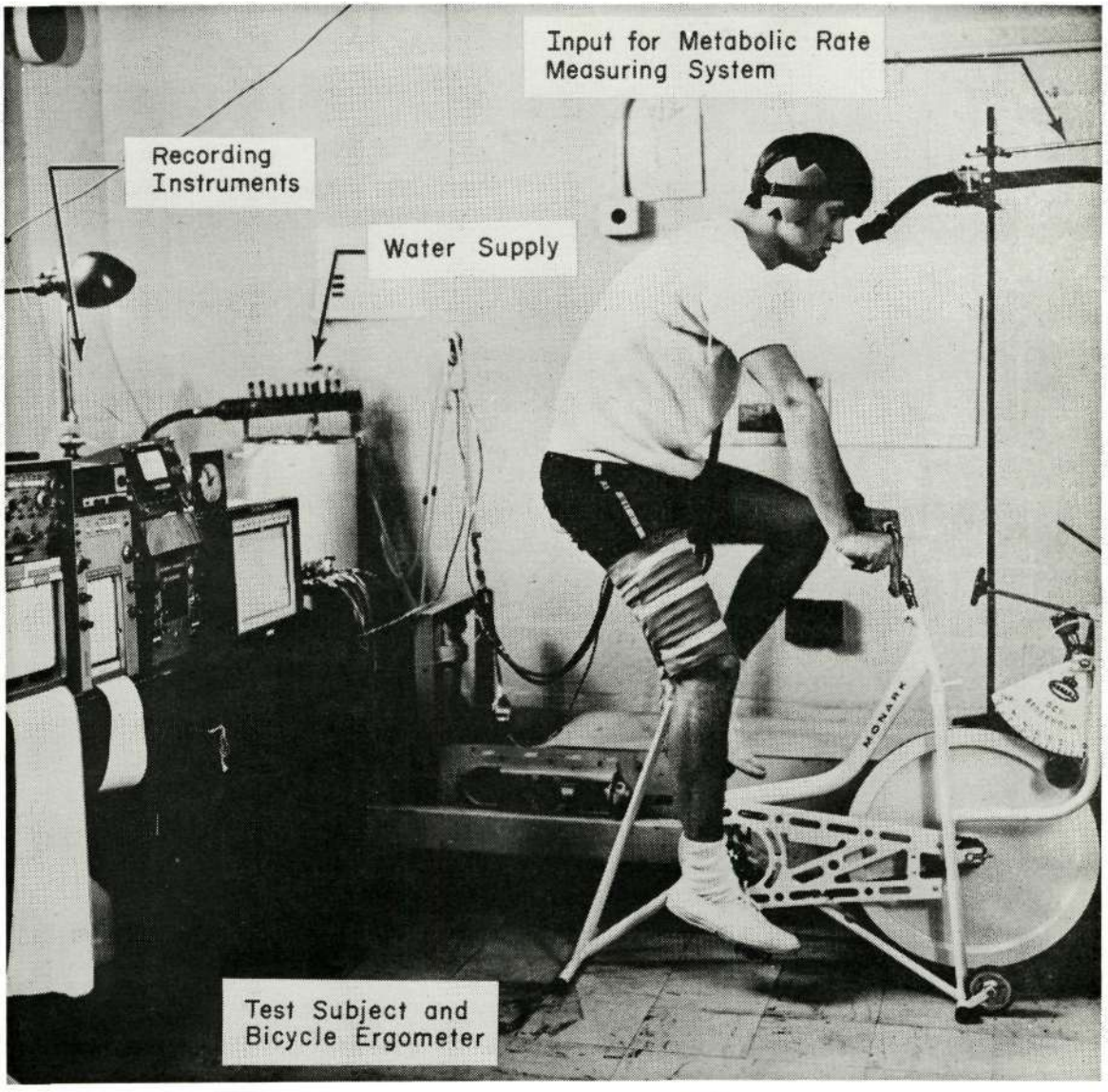

Figure 3.5 General view of the set-up used for the experiments with the individual cooling pads. A test subject is shown pedalling the bicycle ergometer.

TABLE 3.2 CHARACTERISTICS OF SUBJECT TEK

Subject	Age	Height		Weight		Surface Area	
		cm	in.	kg.	lb.	m^2	ft^2
TEK	19	189	74.5	79.7	175.5	2.02	21.7

3.5 RECORDED AND CALCULATED QUANTITIES

3.5.1 Recorded Quantities

During the course of the experiments the following quantities were recorded using the corresponding instrumentation:

1. Temperature distribution on the skin surface between adjacent tubes was measured with No. 30 copper-constantan thermocouples with ice water reference junction and a Leeds and Northrup Speedomax W Potentiometer Recorder.
2. Differential temperature measurement for cooling pad ($T_{inlet}-T_{outlet}$) was made by thermopiles constructed of five copper-constantan thermocouples in series mounted in special plexiglas connectors and a Brush Mark 280 strip chart recorder with high senstivity Brush Pre-Amplifier.
3. Inlet water supply temperature was taken with one copper-constantan thermocouple with ice reference junction and a Brush Mark 280 strip chart recorder with a high sensitivity Brush Pre-Amplifier.
4. Ear canal temperature was measured with an ear thermistor No. 510 and Yellow Springs Instrument Co. Tele-Thermometer with a Brush Mark 220 recorder.
5. Flow rate was measured with a Fischer-Porter No. 48 Rotameter type flow meter.
6. Expired air flow rate was measured with a Parkinson-Cowan

dry gas meter. This flow was measured and collected continuously during transient conditions and periodically during steady state conditions.

7. Oxygen content in expired air was obtained by a Beckman Paramagnetic O_2 analyzer, model C2.
8. CO_2 content in expired air was analyzed with a Godart-Mijnhardt CO_2 thermal conductivity type pulmo analyzer.

3.5.2 Calculated Quantities

1. Total metabolic rate was calculated from the volumetric flow rate of the expired air and the oxygen and CO_2 content obtained from the analysis of this air. The caloric value of oxygen was assumed at 5.0 Kcal/lit [27]. This value, although slightly high, was confirmed by Shitzer, et al., [1] with respiratory quotients found in their experiments. Maximum deviation from the actual caloric value was assumed to be at about 4 percent.
2. The rate of heat removed by each pad was taken as the product of the difference between inlet and outlet temperatures and the coolant flow rate. The specific heat of water was assumed at 1 Btu/lb-°F or 1 Kcal/kg-°C.
3. For the determination of the rate of heat loss by respiration; flow rate, temperature and enthalpy of expired air, assuming it to be saturated, were used.

4. RESULTS AND DISCUSSION

4.1 GENERAL RESULTS

The equipment functioned well throughout the research and the test subject, although overstressed in experiments 9 and 10, was able to complete all of the pre-designed test schedules. TABLE 4.1 outlines the experimental data pertaining to the test subject, the environmental conditions, and each of the variations in the ten experiments. As TABLE 4.1 indicates, the experiments were performed in an environment with the following average conditions:

Pressure	29.35 Hg.
Relative humidity	42 percent
Temperature	71.5°F

Throughout the duration of the ten experiments (approximately six weeks) the test subject maintained an average weight of 176 lb (79.9 kg) although a weight reduction of 1.5 to 3 pounds (0.68 to 1.36 kg) were observed during each of the ten experiments due to loss of body fluid. The test subject's blood pressure and oral temperature remained normal before and after each of the experiments.

The test subject's thigh was cooled with a constant flow (40.5 lb/hr, 18.4 kg/hr) of water at 54.5°F (12.5°C) during all experiments. TABLE 4.2 shows the performance of each test pad for the various experimental conditions. The test subject's metabolic rate shown is the maximum steady state work load that was achieved for each of the experiments. The heat removed by the cooling pad given in the table corresponds to the maximum heat removed from the thigh at the highest steady state work load. The steady state condition was assumed to exist when the temperature profile on the skin surface between the

TABLE 4.1

Experimental Conditions and Measured Data

(Water flow rates and inlet temperatures were identical for all experiments at 40.5 lb/hr and 54.5°F (12.5°C))

Experiment No.	Pad No.	Weight, lb		Blood Pressure		Oral Temp, °F		Pressure in. Hg.	Relative Humidity	Temperature °F
		Before	After	Before	After	Before	After			
1	2	176.83	175.25	120/80	120/80	98.5	97.6	29.38	42	72
2	2	177.66	177.52	120/80	120/90	98.2	98.4	29.32	41	72
3	2	176.40	175.60	125/80	125/80	98.4	98.2	29.38	43	71
4	1	179.68	177.34	120/65	120/90	97.6	98.0	29.32	40	73
5	2	178.36	176.60	120/80	120/80	97.8	98.2	29.30	41	72
6	3	176.06	175.12	120/80	120/80	97.8	98.4	29.50	43	73
7	2	175.71	174.12	115/60	120/70	97.7	98.6	29.52	40	72
8	3	176.54	174.09	120/80	120/80	97.6	98.2	29.44	42	70
9	2	173.36	170.39	110/80	120/80	98.3	98.5	29.30	43	73
10	3	175.92	172.50	110/80	110/80	98.4	98.0	29.41	43	72

TABLE 4.2

Heat Removed by Cooling Pads During Maximum Steady State Metabolic Rates						
Experiment	Pad	Maximum Steady State Total Metabolic Rate of Subject		Heat Removed by Pad During Steady State		Percent of Total Removed by Pad
		Btu/hr	w	Btu/hr	w	
1	2	200	59	-- *	*	-- *
2	2	320	94	148	44	46**
3	2	600	176	183	54	30
4	1	900	264	185	54	20
5	2	900	264	190	56	21
6	3	900	264	208	61	23
7	2	1800	528	290	85	16
8	3	1800	528	300	88	17
9	2	1800	528	290	85	16
10	3	1800	528	300	88	17

*Steady state temperature profile was not attained.
**Questionable value.

cooling tubes was fully developed and did not change as a function of time.

4.2 TEMPERATURE DISTRIBUTIONS FOR SITTING, STANDING AND MILD WORK

Cooling pad No. 2 was used for experiments 1, 2, and 3. The objective of these experiments was to investigate the nature of the human thigh's response to cooling by a pad with a constant water temperature and flow rate but for three activity levels. Figure 4.1 illustrates the results of experiments 1, 2, and 3. For each experiment there is one set of data consisting of two lines. These approximately parallel lines represent the highest and lowest temperatures which occured on the skin surface between two adjacent cooling tubes. The higher temperature line represents a point on the skin surface equidistant between the cooling tubes, and the lower temperature line represents a point on the skin surface immediately adjacent to the cooling tube. The difference between the input water temperature and the temperature of the water that leaves the pad is also plotted.

TABLE 4.3 summarizes the information which is presented in Fig. 4.1. As illustrated, a steady state condition was never achieved in experiment No. 1. After three hours the temperature on the skin surface of the thigh was still decreasing at a fairly steady rate of 1.35°F (0.75°C) per hour. The metabolic rate of the sitting test subject remained constant at 200 Btu/hr (59 w). It should be noted that this measured value of 200 Btu/hr (59 w) is about 75 to 100 Btu/hr below average for a sitting individual.

In experiment No. 2 all of the experimental parameters remained

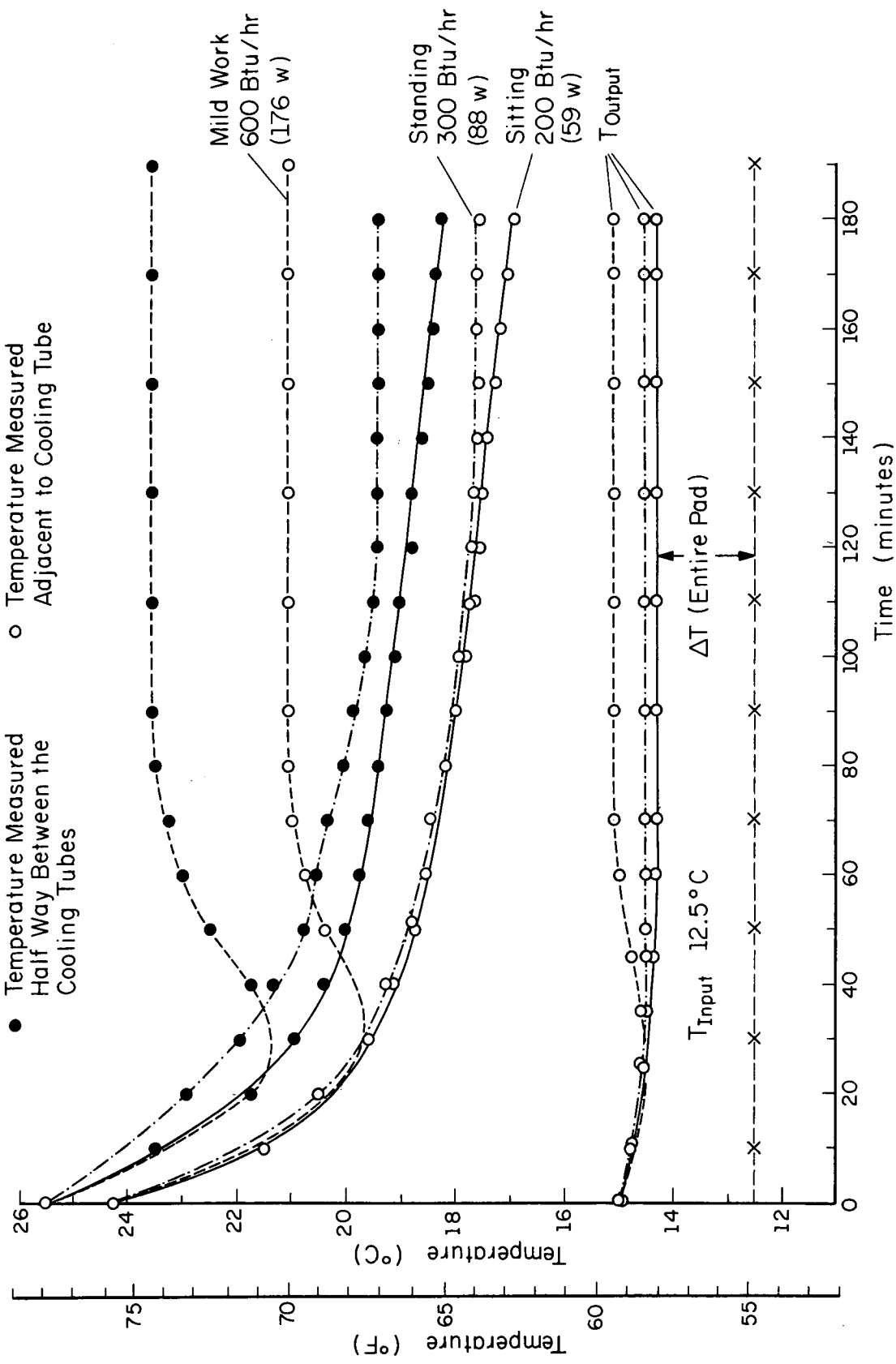

Figure 4.1 Results of experiments 1, 2, and 3 using cooling pad No. 2 with constant experimental conditions and varying work load.

TABLE 4.3

Summary of the Results of Experiments 1, 2, and 3 with Pad No. 2

Experiment Number	Highest Metabolic Rate Reached by Subject During Steady State Conditions		Approximate Time to Reach Steady State Temperature Profile, min.	Difference Between Highest and Lowest Temperatures at Steady State		Temperature Rise Across Pad, $T_{in} - T_{out}$ at Steady State		Heat Removed by Pad at Steady State	
	Btu/hr	w		°F	°C	°F	°C	Btu/hr	w
1	200*	59	>180	---	---	---	---	---	---
2	320	94	130	3.40	1.89	3.6	2.00	142	41**
3	600	176	90	4.50	2.50	4.7	2.61	185	54

*Steady state profile was not attained.
**Questionable value.

the same as in experiment No. 1 with the exception of the test subject's metabolic rate. The standing position was employed and the resulting metabolic rate was 320 Btu/hr (94 w), 120 Btu/hr (35 w) higher than in the case of sitting. This time the temperature distribution on the surface of the thigh did reach a steady state in approximately 130 minutes. During the steady state condition a maximum temperature difference of 3.4°F (1.9°C) was observed on the skin surface. At the same time a total temperature rise of 3.6°F (2.0°C) was recorded for the water supply. At a work load of 320 Btu/hr (94 w) this temperature difference corresponded to a heat removal rate of 142 Btu/hr (41 w).

An assumption was made that a mild work activity level would correspond to twice the metabolic rate of standing. This mild work was simulated by an activity level of 600 Btu/hr (176 w). During experiment No. 3 the test subject reached a steady state temperature distribution in 90 minutes while working at 600 Btu/hr (176 w). The maximum temperature difference on the skin surface during steady state was 4.5°F (2.5°C). At steady state the heat removed from the thigh by the cooling pad was 185 Btu/hr (54 w) corresponding to a water temperature rise of 4.7°F (2.6°C). It should be noted that the highest temperature recorded between adjacent tubes rose from 67.1°F (19.5°C) at 320 Btu/hr (94 w) in experiment No. 2 to 74.3°F (23.5°C) at 600 Btu/hr (176 w) in experiment No. 3.

At the beginning of experiments 1, 2, and 3 the cooling pad was strapped on the subject's thigh while cooling water was flowing through the pad. In later experiments the pad was placed on the thigh and the subject was then allowed to rest for 30 minutes.

During this time the thigh came to equilibrium with no flow in the cooling pad. Cooling fluid was introduced only after the thigh had reached a steady state without cooling. This procedure was instituted in order to gain some additional insight as to the course of change of the skin temperature on the surface of the thigh during the onset of cooling.

4.3 COMPARISON OF THE SURFACE TEMPERATURE TRANSIENTS FOR THE THREE PADS

During experiments 4, 5, and 6, cooling pads 1, 2, and 3 were tested, respectively. During each of these experiments the inlet water temperature was maintained constant at 54.5°F (12.5°C); the flow rate was maintained constant at 40.5 lb/hr (18.4kg/hr) and the activity level of the test subject was monitored and regulated at 900 Btu/hr (264 w).

Figure 4.2 illustrates the result of experiments 4, 5, and 6 and these results are also summarized in TABLE 4.4. As is shown, the cooling pad was placed on the test subject at t = 0. He was allowed to rest for the first 30 minutes after which the cooling fluid was introduced. The temperature profile on the skin surface decreased afterward. The transient times to reach steady state were 90 minutes for pad No. 2 and 100 minutes for pads No. 1 and 3. It is interesting to note that at steady state the temperature distributions for pads No. 1 and 3 almost coincide while the temperature profile for pad No. 2 is noticably lower by about 3.5°F (2°C). This observation can be accounted for by the fact that pad No. 2 has a higher cooling tube density than pads No. 1 and 3. This high tube density is also reflected in a skin temperature differential of

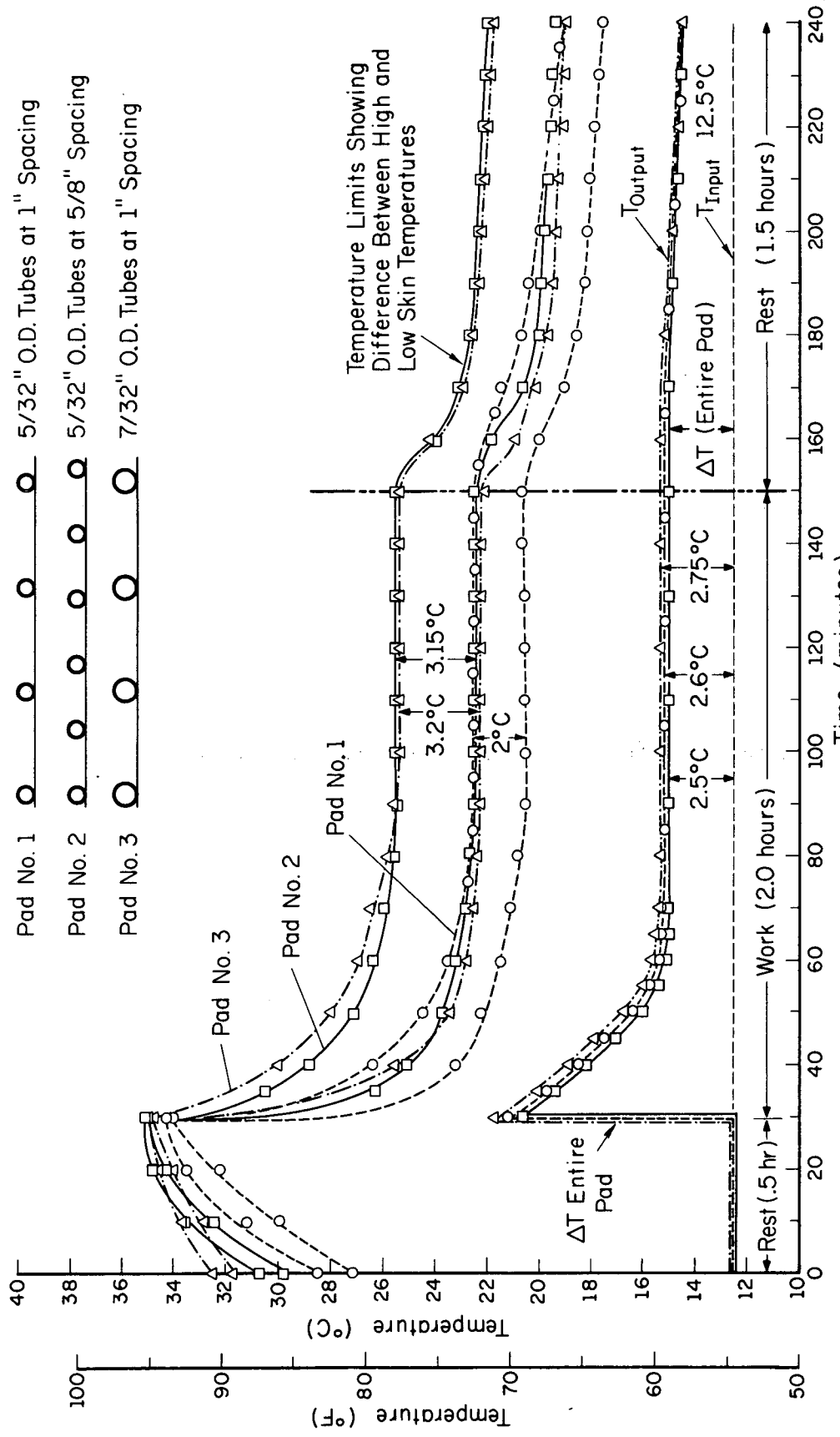

Figure 4.2 Results of experiments 4, 5, and 6 with constant experimental conditions and constant metabolic rate 900 Btu/hr (264 w).

TABLE 4.4

Results of Experiments 4, 5, and 6 with Constant Metabolic Rate of 900 Btu/hr (257 w) Using Pads 1, 2, and 3

Experiment	Pad	Highest Metabolic Rate at Steady State		Time to Develop Steady State Temperature Profile, min.	Highest Skin Temperature		Lowest Skin Temperature		$T_h - T_{low}$		ΔT Pad		Heat Removed by Pad	
		Btu/hr	w		°F	°C	°F	°C	°F	°C	°F	°C	Btu/hr	w
4	1	900	264	100	78.1	25.6	70.61	21.4	10.2	5.67	4.5	2.5	185	54
5	2	900	264	90	72.3	22.4	68.7	20.4	6.5	3.6	4.7	2.6	190	56
6	3	900	264	100	77.7	25.4	71.9	22.2	10.3	5.7	4.95	2.75	208	61

only 3.6°F (2°C) for pad No. 2 while the differences between the high and low skin temperatures for pads No. 1 and 3 are 5.67°F (3.15°C) and 5.76°F (3.2°C), respectively. Consequently, while pad No. 2 provided a lower skin temperature in general, it also provided a more uniform skin temperature profile between the tubes. With a work load of 900 Btu/hr (264 w), pad No. 3 removed the highest amount of heat; i.e., 208 Btu/hr (61 w) corresponding to a cooling fluid temperature difference of 4.95°F (2.75°C).

4.4 COMPARISON OF THE STEADY STATE SKIN SURFACE TEMPERATURE DISTRIBUTIONS FOR THE THREE PADS

Steady state temperature distributions on the skin corresponding to activity levels of 300 Btu/hr (88 w), 900 Btu/hr (264 w), and 1800 Btu/hr (528 w) are shown in Figs. 4.3, 4.4, and 4.5, respectively. The results for pad No. 1 are shown in Fig. 4.4 alone since this pad was used during experiment No. 4 only (mild work, 900 Btu/hr, TABLE 4.2).

All profiles shown in these figures resemble bell-shaped curves. The same qualitative results have been obtained by Chato and co-workers [7]. In general, the profiles obtained from pad No. 2 were the flattest and also lowest in temperatures. These results are due to the higher tube density of pad No. 2 as compared to the other two pads.

Temperatures immediately underneath the cooling tubes could not be accurately obtained with the present measuring technique. Thus, only measured skin temperatures in the region not in contact with the cooling tubes, i.e., $\beta < z/a < (2 - \beta)$, are shown in Figs. 4.3,

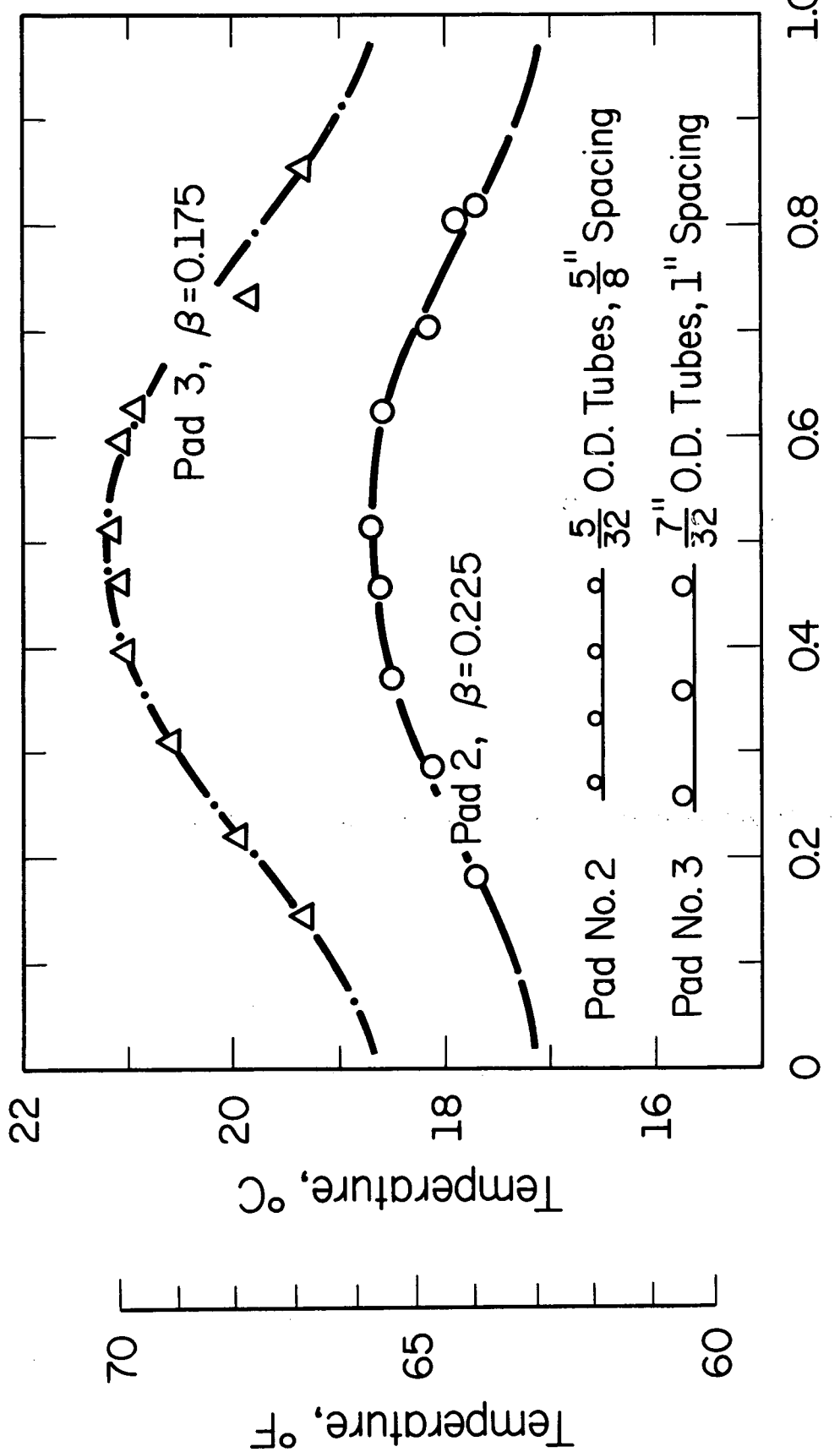

Figure 4.3 Steady state temperature distribution for pads 2 and 3 under constant experimental conditions and constant metabolic rate at 300 Btu/hr (88 w).

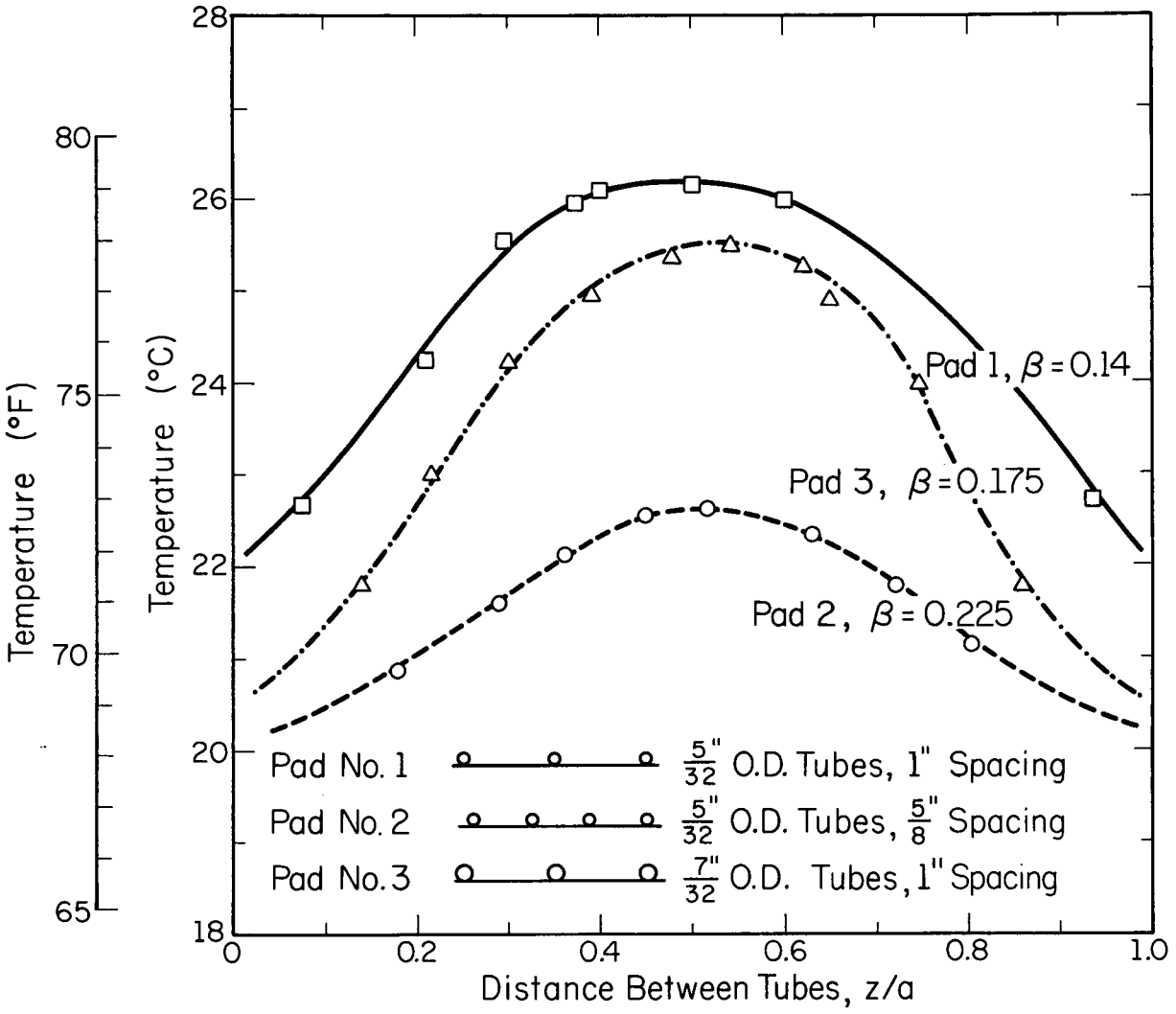

Figure 4.4 Steady state temperature distribution for pads 1, 2, and 3 under constant experimental conditions and constant metabolic rate at 900 Btu/hr (264 w).

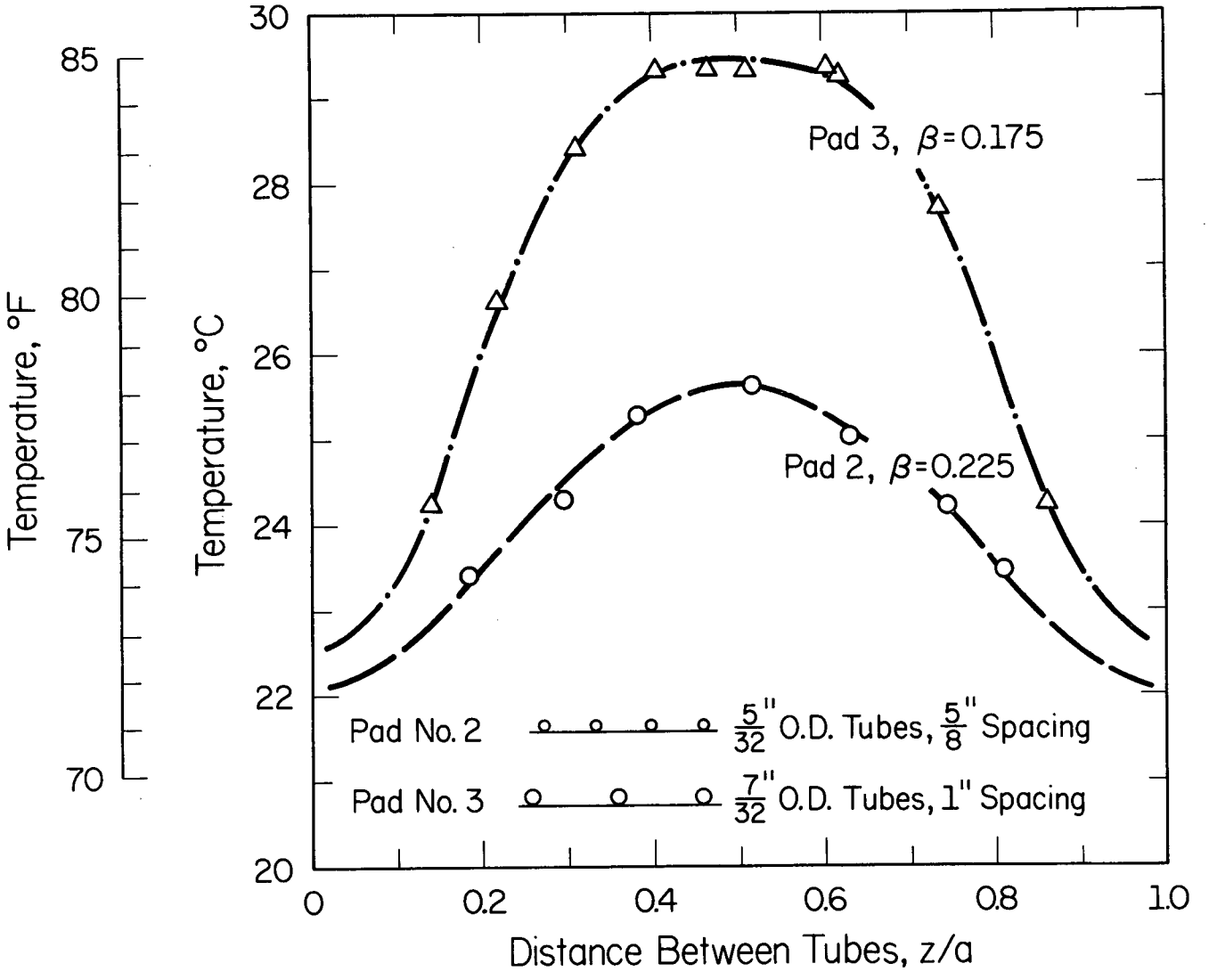

Figure 4.5 Steady state temperature distribution for pads 2 and 3 under constant experimental conditions and constant metabolic rate at 1800 Btu/hr (528 w).

4.4, and 4.5. The profiles in these figures were extrapolated into the areas covered by the cooling strips, too. The extrapolated values could not be verified and should be treated as estimates only.

4.5 COMPARISON OF THE STEADY STATE SURFACE TEMPERATURE DISTRIBUTIONS WITH ANALYTICAL RESULTS

Analytical expressions for the steady state temperature distribution on the skin surface between adjacent cooling tubes for the tissue modeled as a rectangular slab or a cylindrical shell are given in Ref. [1] by Eqs. (5.1) and (E.2) (with $r = R_2$), respectively. Following is a list of parameters appearing in those equations that affect the temperature distribution:

(1) Temperature of the inner core and the arterial blood, $T_1 = T_a$,

(2) Specific heat of blood, c_b,

(3) Thermal conductivity of the tissue, k,

(4) Ratio of cooling tube width to cooling tube spacing, β,

(5) Cooling tube spacing, $2\bar{a}$,

(6) Average heat flux at skin surface, f_a,

(7) Number of terms used in the series computation, n,

(8) Depth of tissue, b,

(9) Shape of the flux function, f(z),

(10) Average rate of heat generated per unit volume of tissue, q_m,

(11) Average blood perfusion rate per unit volume of tissue, w_b, and, in the cylindrical model only due to the additional degree of freedom,

(12) Radius of cylindrical shell, R_1 or R_2.

The first eight of these parameters and the radius of the cylindrical shell could either be measured or estimated with a fair degree of accuracy. The remaining three, i.e., $f(z)$, q_m, and w_b, were not measured in the present work and were left to be estimated by the method of fitting theoretical curves to the experimental data. Curve fitting was done with the aid of a digital computer. Equations (5.1) and (E.2) of Ref. [1] were programmed and temperature profiles were computed for various combinations of the above three parameters. The computer output was then analyzed to determine that combination of parameters which yielded curves fitting closest with the experimental data. Simultaneously, the parameters and the corresponding temperature profiles were checked against the following criteria:

(1) The lowest temperature on the skin (immediately underneath the cooling tube) should not be below the temperature of the cooling water; in all experiments coolant temperature was maintained at 54.5°F (12.5°C).

(2) Blood perfusion and heat generation rates per unit volume of tissue should not exceed values found in the literature.

(3) Only temperatures measured on the skin away from the cooling tubes were considered for the comparison.

In addition, the following two assumptions were made:

(1) An estimated 25 to 30 Btu/hr (7.3 to 8.7 w) of the total heat removed by the cooling pads were gained from the environment.

2-2

(2) Some heat was removed through the air gap along the areas not in contact with the cooling tubes. A parameter, η, denoting the ratio of heat fluxes at the uncontacted to that at the contacted areas was introduced. This ratio was usually assumed at about 10 percent.

A large number of combinations of the above parameters over a wide range were considered. Results for pads No. 2 and 3 at the high metabolic rate of 1800 Btu/hr (528 w) are shown in Figs. 4.6 and 4.7, respectively. In these figures comparison is made between the experimental results and both the cylindrical and rectangular models. The agreement between experimental and theoretical results is quite good, particularly for pad No. 2. Also, as can be observed, no significant differences exist between the cylindrical and rectangular models. It should, however, be noted that the curves presented in Figs. 4.6 and 4.7 are not unique; nor are the parameters that yielded those curves to be regarded as representing the true physiological values. The only objective that we had in mind while attempting the fitting of analytical curves to measured data was to explore whether a reasonable correspondence could be obtained. Anything beyond this specific objective is not implied. Improved techniques for measuring the unknown parameters and skin temperatures are required to render the comparison between measured and analytically predicted results more meaningful.

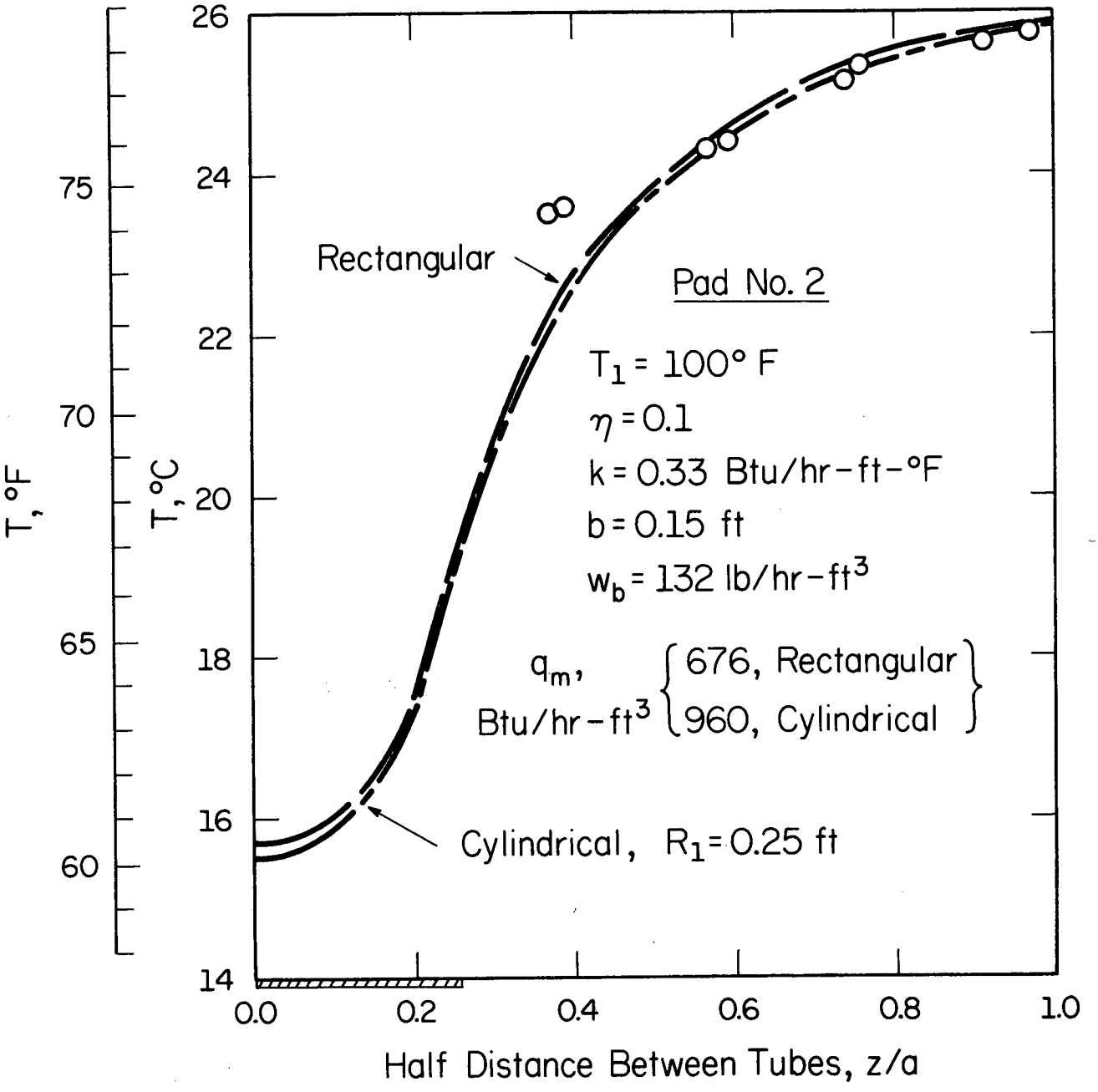

Figure 4.6 Comparison of analysis with experimental results for cooling pad No. 2. Metabolic rate 1800 Btu/hr (528 w).

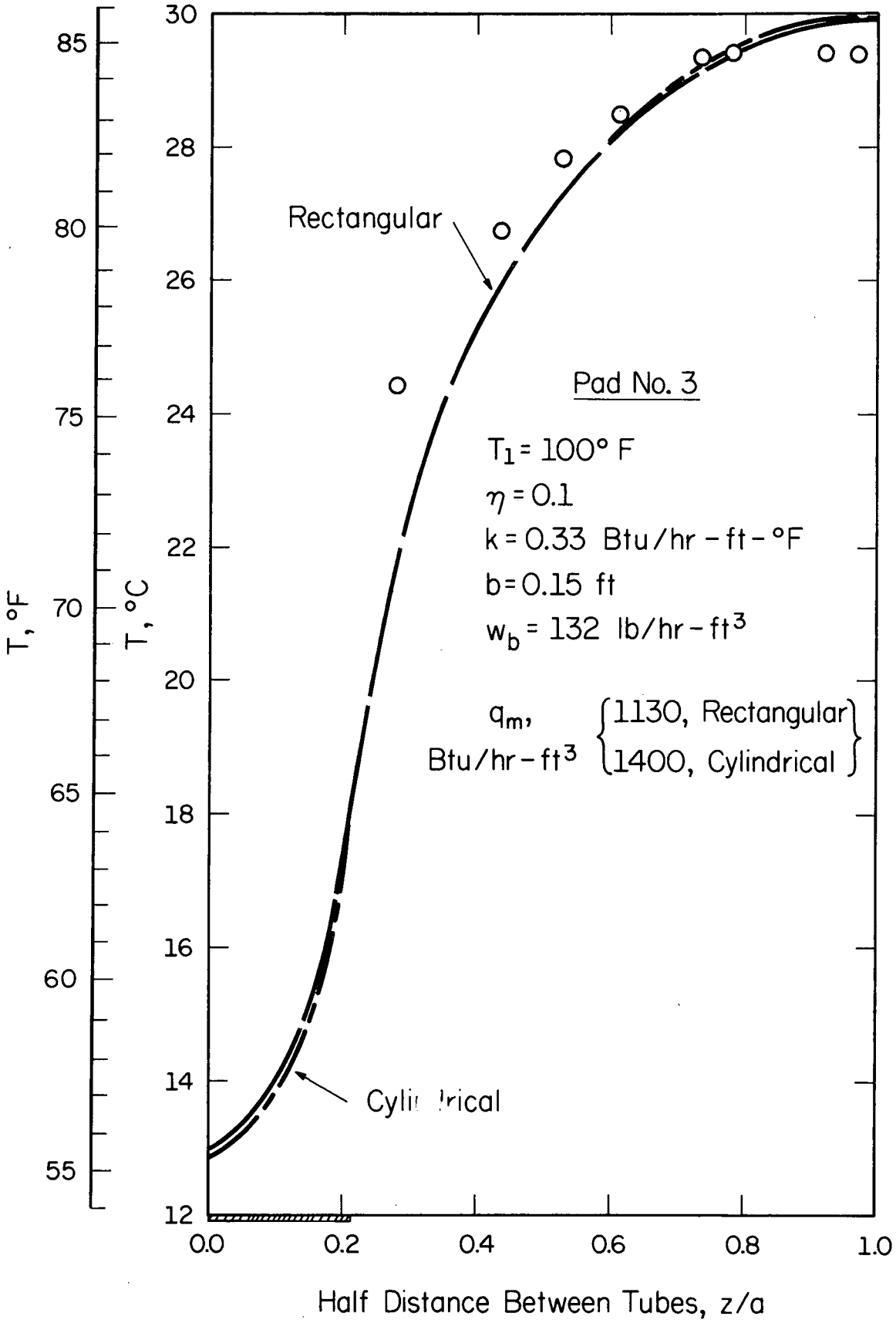

Figure 4.7 Comparison of analysis with experimental results for cooling pad No. 3. Metabolic rate 1800 Btu/hr (528 w).

4.6 RESULTS OF TRANSIENT EXPERIMENTS

In experiments 7 and 8 the transient response due to a large and sudden increase in metabolic rate was studied. As shown in Fig. 4.8, the test subject stood for about three hours in order to reach a steady state temperature distribution on the skin surface. With the flow rate and input water temperature held constant, the metabolic heat generation rate was then raised from 300 Btu/hr (88 w) to 1800 Btu/hr (528 w). As can be seen, the transition in metabolic rate from low to high activity level occurred in about five minutes. The test subject maintained the 1800 Btu/hr (528 w) activity level for 90 minutes. At this time he was allowed to rest and his metabolic rate returned to 300 Btu/hr (88 w) in about ten minutes.

The transient response of the skin surface temperature profile corresponding to sudden change in the total metabolic rate was recorded for pads No. 2 and 3 in experiments 7 and 8, respectively. Figures 4.9 and 4.10 show the results of experiment 7. Figure 4.9 shows the course of change of the temperature profile on the skin surface between adjacent cooling tubes. The lowest curve at $t = 0$ represents the fully developed temperature profile at 300 Btu/hr (88 w) and the highest curve at $t = 40$ min represents the fully developed profile corresponding to an activity level of 1800 Btu/hr (528 w). The curves at $t = 10$ min and $t = 20$ min are plotted at the intermediate stages and show the nature of the development of the temperature profile.

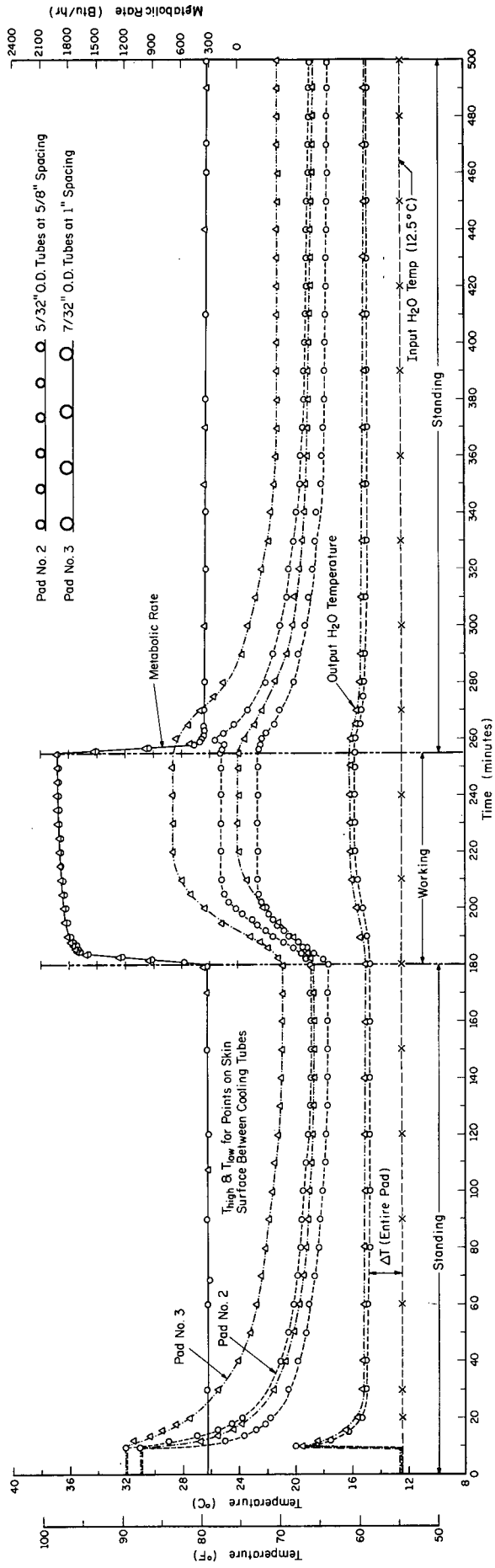

Figure 4.8 Results of experiments 7 and 8.

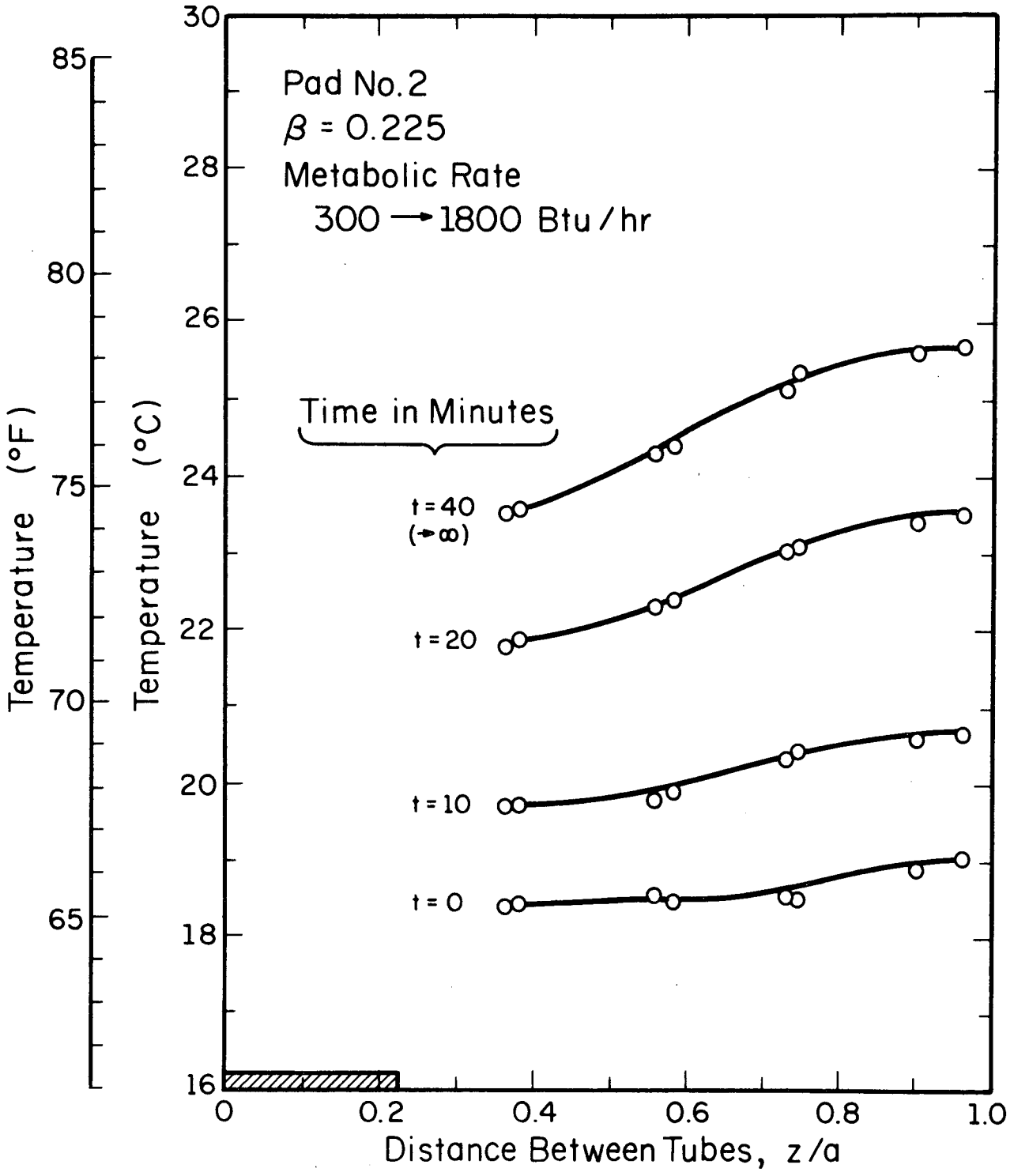

Figure 4.9 Development of temperature profile on the skin for pad No. 2 resulting from an increase in metabolic rate from 300 to 1800 Btu/hr (88 to 528 w).

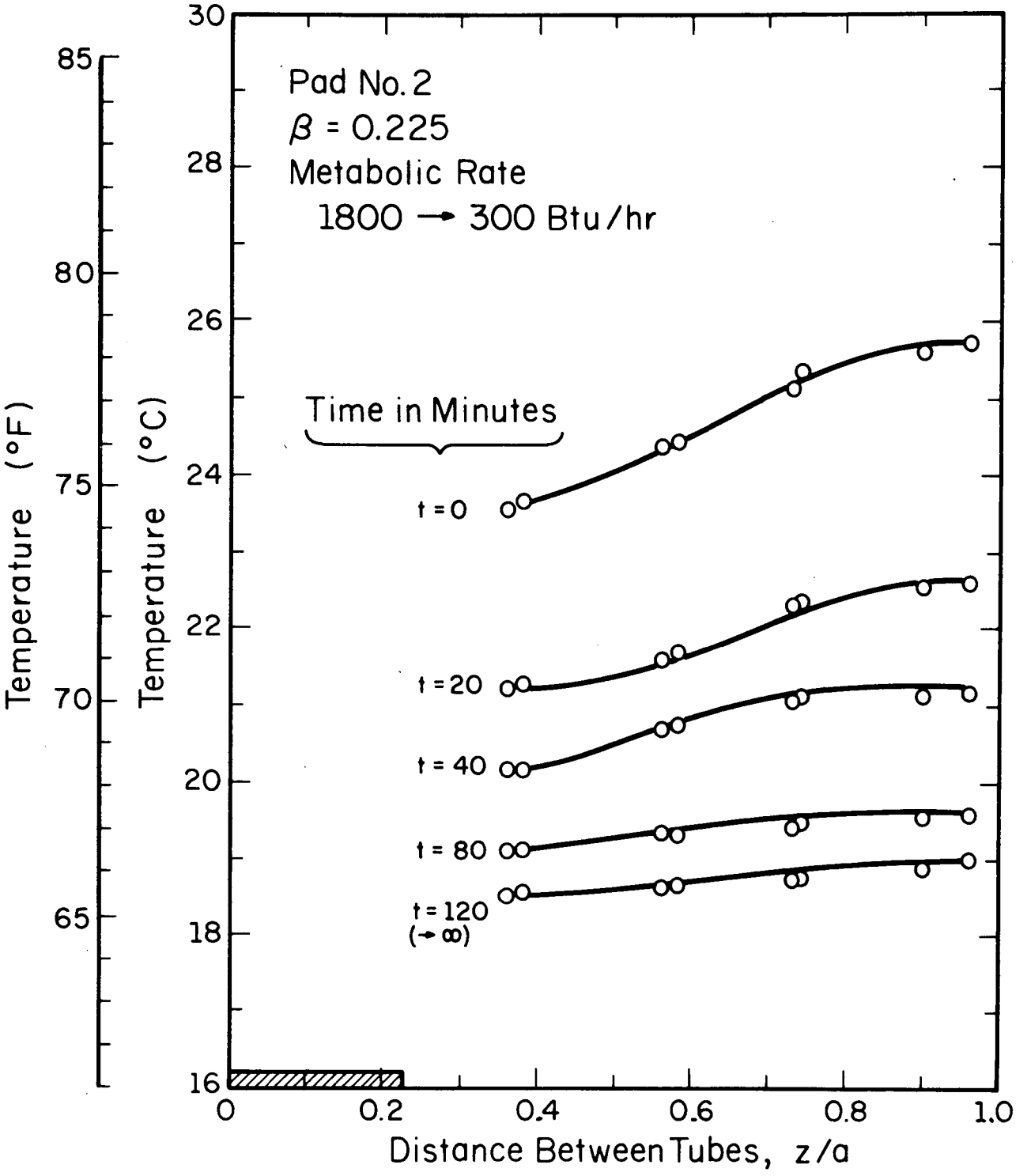

Figure 4.10 Development of temperature profile on the skin for pad No. 2 resulting from a decrease in metabolic rate from 1800 to 300 Btu/hr (528 to 88 w).

Figure 4.10 shows the course of change of the temperature profile as it changed with a decrease in metabolic rate from 1800 Btu/hr (528 w) to 300 Btu/hr (88 w). In this case the highest curve at t = 0 represents the fully developed temperature profile at 1800 Btu/hr (528 w). The lower curve at t = 120 represents the temperature profile at steady state corresponding to a metabolic activity rate of 300 Btu/hr (88 w). The intermediate values at t = 20, 40, 60 and 80 minutes show the nature of the development of the lower temperature profile.

In the case of the increasing metabolic rate the temperature distribution reaches a steady state in 40 minutes for pad No. 2. However, a decrease in the total metabolic rate over the same range results in a transient time of 120 minutes to reach steady state for the same pad. Thus, it takes about three times as long to reach steady state when changing from a high to a low metabolic rate as compared to changing from a lower to a higher rate for pad No. 2.

The results of experiment 8 (using pad No. 3) are shown in Figs. 4.11 and 4.12. In these figures the same scheme was used to present the data as in Figs. 4.9 and 4.10. Figure 4.11 represents the change in the temperature profile for an increasing metabolic rate and Fig. 4.12 represents the change for a decreasing metabolic rate. Again, the metabolic rates ranged from 300 Btu/hr (88 w) at the low end to 1800 Btu/hr (528 w) at the high end. TABLE 4.5 summarizes the results of experiments 7 and 8 and can be used to compare the performance of pads No. 2 and 3.

The temperature profile develops slightly faster for pad No. 2 at 40 minutes as compared with a time of 60 minutes for pad No. 3

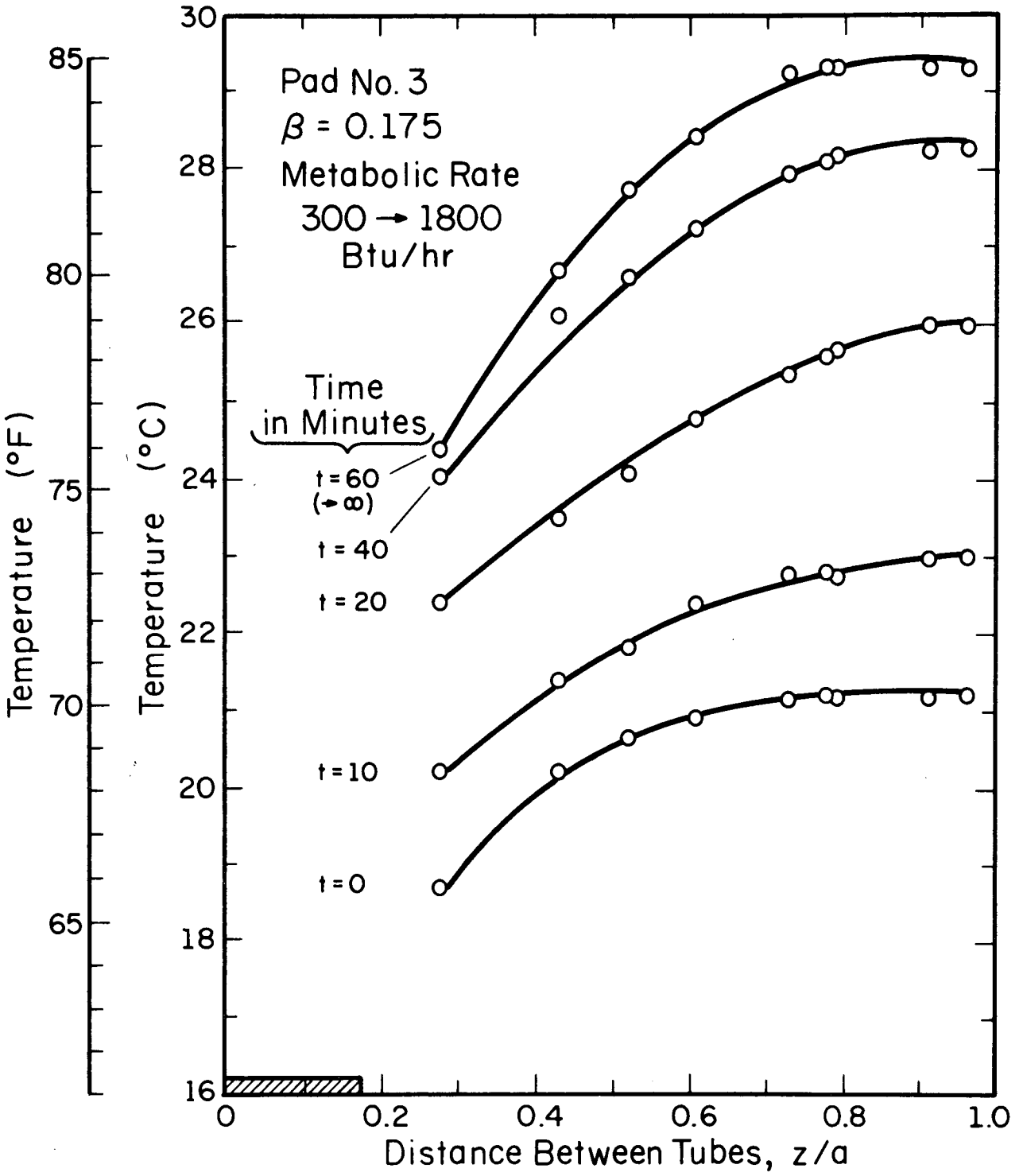

Figure 4.11 Development of temperature profile on the skin for pad No. 3 resulting from an increase in metabolic rate from 300 to 1800 Btu/hr (88 to 528 w).

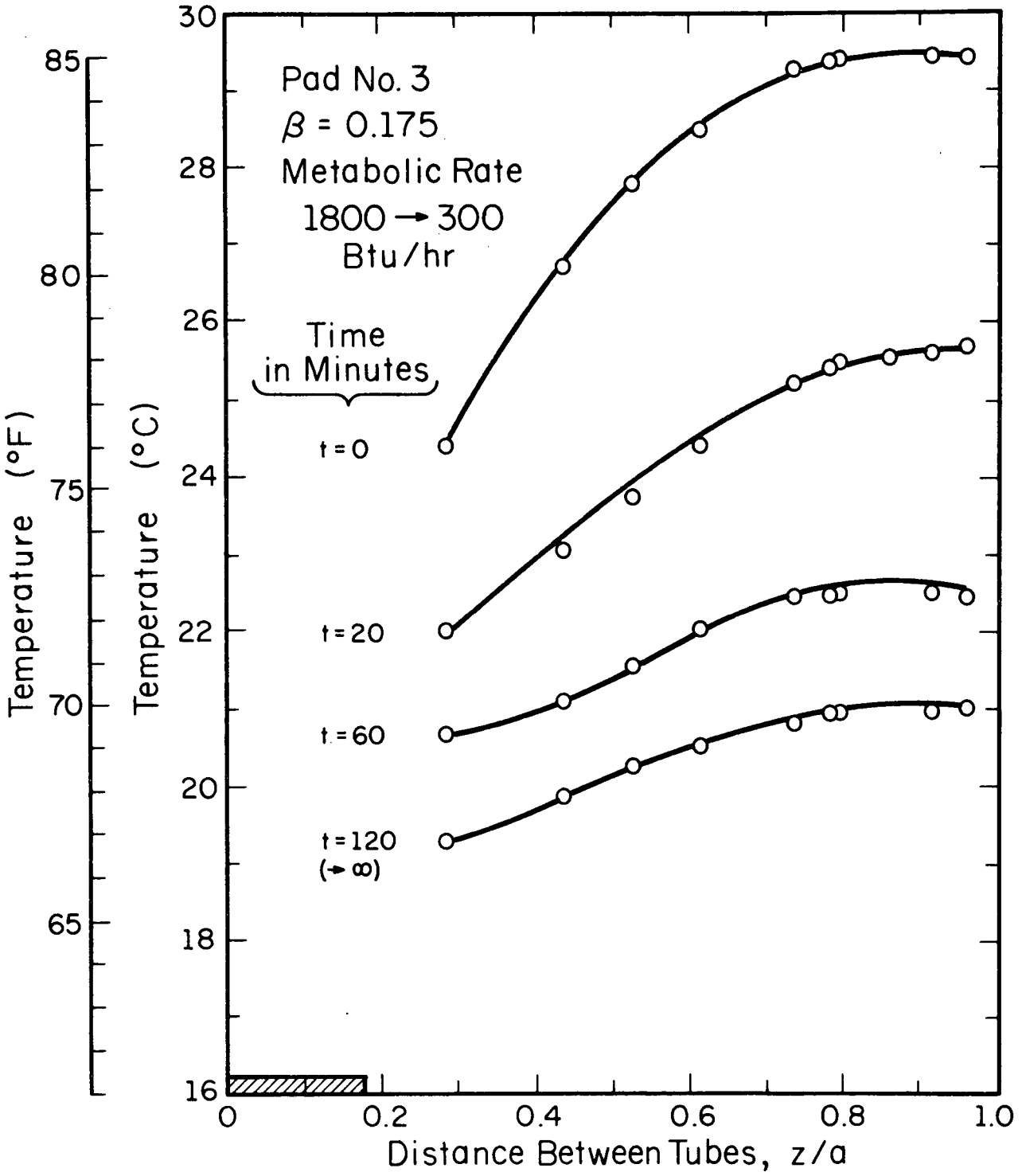

Figure 4.12 Development of temperature profile on the skin for pad No. 3 resulting from a decrease in metabolic rate from 1800 to 300 Btu/hr (528 to 88 w).

TABLE 4.5

Results of Experiments 7 and 8

(Flow rate and water temperature remained constant)

Experiment	Pad	Change in Metabolic Rate Btu/hr	Change in Metabolic Rate w	Time to Reach Steady State Profile, Min.
7	2	300 → 1800	88 → 528	40
8	3	300 → 1800	88 → 528	60
7	2	1800 → 300	528 → 88	120
8	3	1800 → 300	528 → 88	120

for an increasing metabolic rate. The time for the temperature profile development was equal for both pads in the case of a decreasing metabolic rate. Comparison of Figs. 4.9 and 4.11 reveals that the temperature profile is both lower and flatter for pad No. 2 as compared with pad No. 3. Also, the profile was shifted about 12.5°F (7°C) for pad No. 2 compared with a 16°F (9°C) shift for pad No. 3, for the case of increasing and decreasing metabolic rates.

In general then, pad No. 2 provided a lower, more uniform temperature distribution. This temperature distribution also proved to be more stable and did not shift as much as in the case of pad No. 3 under identical conditions of change. This probably is the major factor in accounting for a smaller time constant for pad No. 2 as compared with pad No. 3.

The results for experiments 9 and 10 are shown in Fig. 4.13. As illustrated in Fig. 4.13, the skin temperatures were monitored

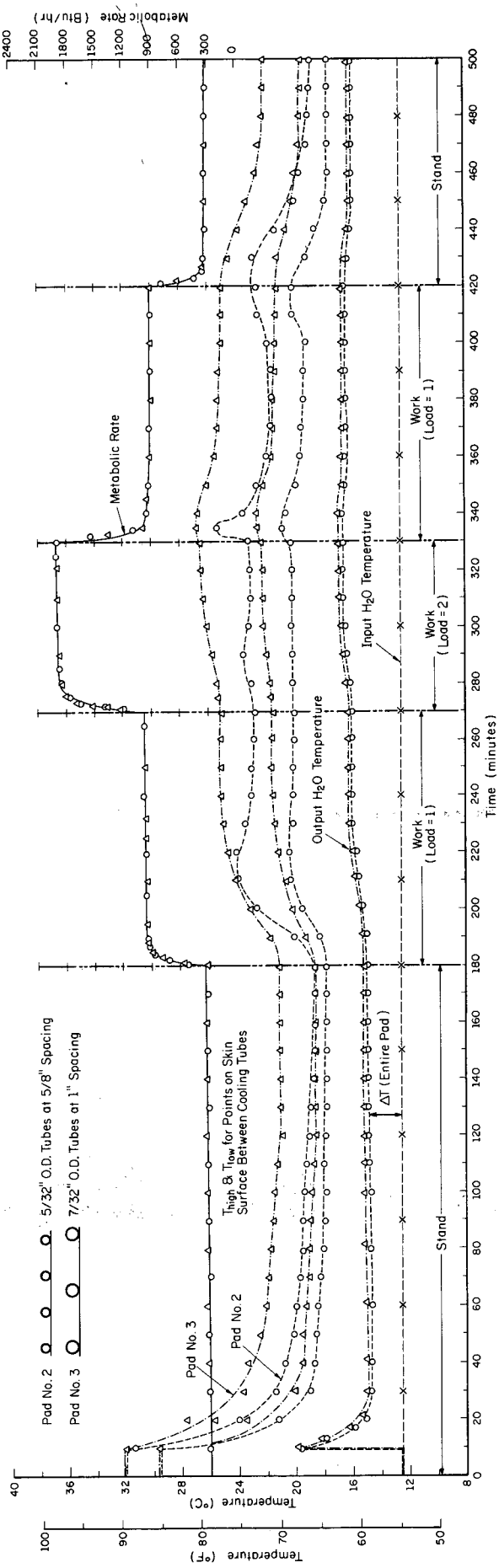

Figure 4.13 Results of experiments 9 and 10.

for pads No. 2 and 3 for several transient metabolic conditions. The transient intervals analyzed were as follows: increasing metabolic rates for pads No. 2 and 3 from:

1. 300 Btu/hr (88 w) to 900 Btu/hr (264 w),
2. 900 Btu/hr (264 w) to 1800 Btu/hr (528 w)

and reversed sequence of decreasing metabolic rates for pads No. 2 and 3 from

3. 1800 Btu/hr (528 w) to 900 Btu/hr (264 w)
4. 900 Btu/hr (264 w) to 300 Btu/hr (88 w).

Again, it can be noted that the test subject required very little time to reach a steady metabolic rate for each new activity. This fact supports the initial assumption that changes in metabolic rates can be regarded as step functions as compared to changes in temperature.

There are relatively short duration increases in temperature occurring at the beginning of some of the work loads, particularly after a reduction in metabolic rate. The rapidity of this change indicates a physiological response of some kind, such as a sudden reduction in blood flow.

Figure 4.14 shows the course of change for the temperature profile reacting to changes from low to moderate and to high metabolic activity levels for pad No. 2. Figure 4.15 shows the nature of the temperature distributions as the metabolic rate decreases from high to low.

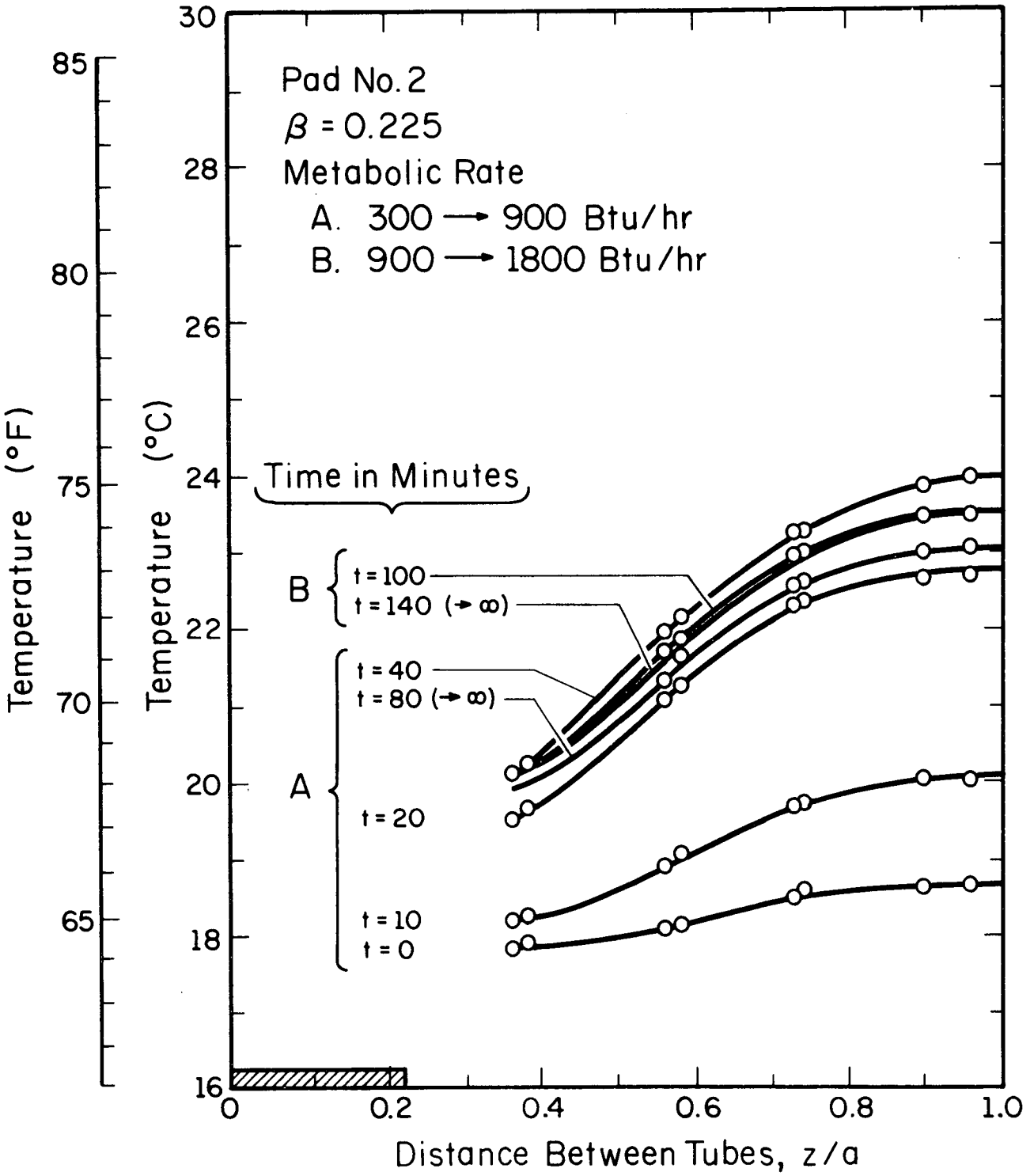

Figure 4.14 Development of temperature profile on the skin for pad No. 2 resulting from increases in metabolic rates from 300 to 900 Btu/hr (88 to 264 w) and from 900 to 1800 Btu/hr (264 to 528 w).

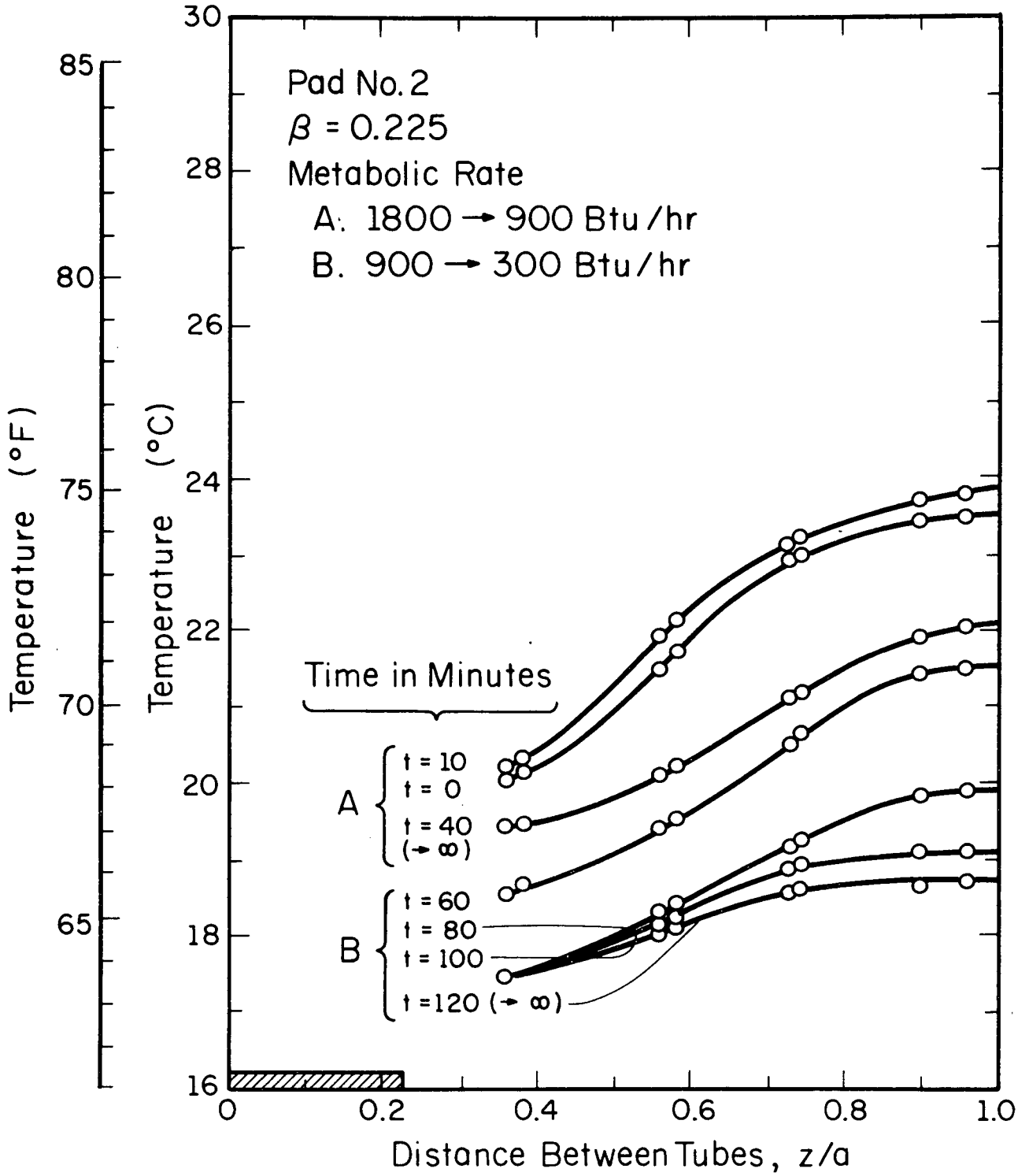

Figure 4.15 Development of temperature profile on the skin for pad No. 2 resulting from decreases in metabolic rates from 1800 to 900 Btu/hr (528 to 264 w) and from 900 to 300 Btu/hr (264 to 88 w).

The results of experiment 10 are shown in Figs. 4.16 and 4.17. In this case pad No. 3 was tested and the temperature distributions were measured in accordance with changes in metabolic activity from low to high and from high to low. The results of experiments 9 and 10 are presented in summary form in TABLE 4.6. It can be seen that both pads No. 2 and 3 required a time of 80 minutes to reach a steady state temperature distribution in accordance with an increase in metabolic activity from 300 to 900 Btu/hr (88 w to 264 w). Similarly, pads No. 2 and 3 also required an additional time of sixty minutes to reach steady state with an increase in metabolic rate from 900 Btu/hr to 1800 Btu/hr (264 w to 528 w).

TABLE 4.6

Results of Experiments 9 and 10

(Flow rates and input water temperatures held constant)

Experiment	Pad	Change in Metabolic Rate Btu/hr	Change in Metabolic Rate w	Time to Reach Steady State Profile, min.
9	2	300 → 900	88 → 264	80
10	3	300 → 900	88 → 264	80
9	2	900 → 1800	264 → 528	60
10	3	900 → 1800	264 → 528	60
9	2	1800 → 900	528 → 264	40
10	3	1800 → 900	528 → 264	80
9	2	900 → 300	264 → 88	80
10	3	900 → 300	264 → 88	60

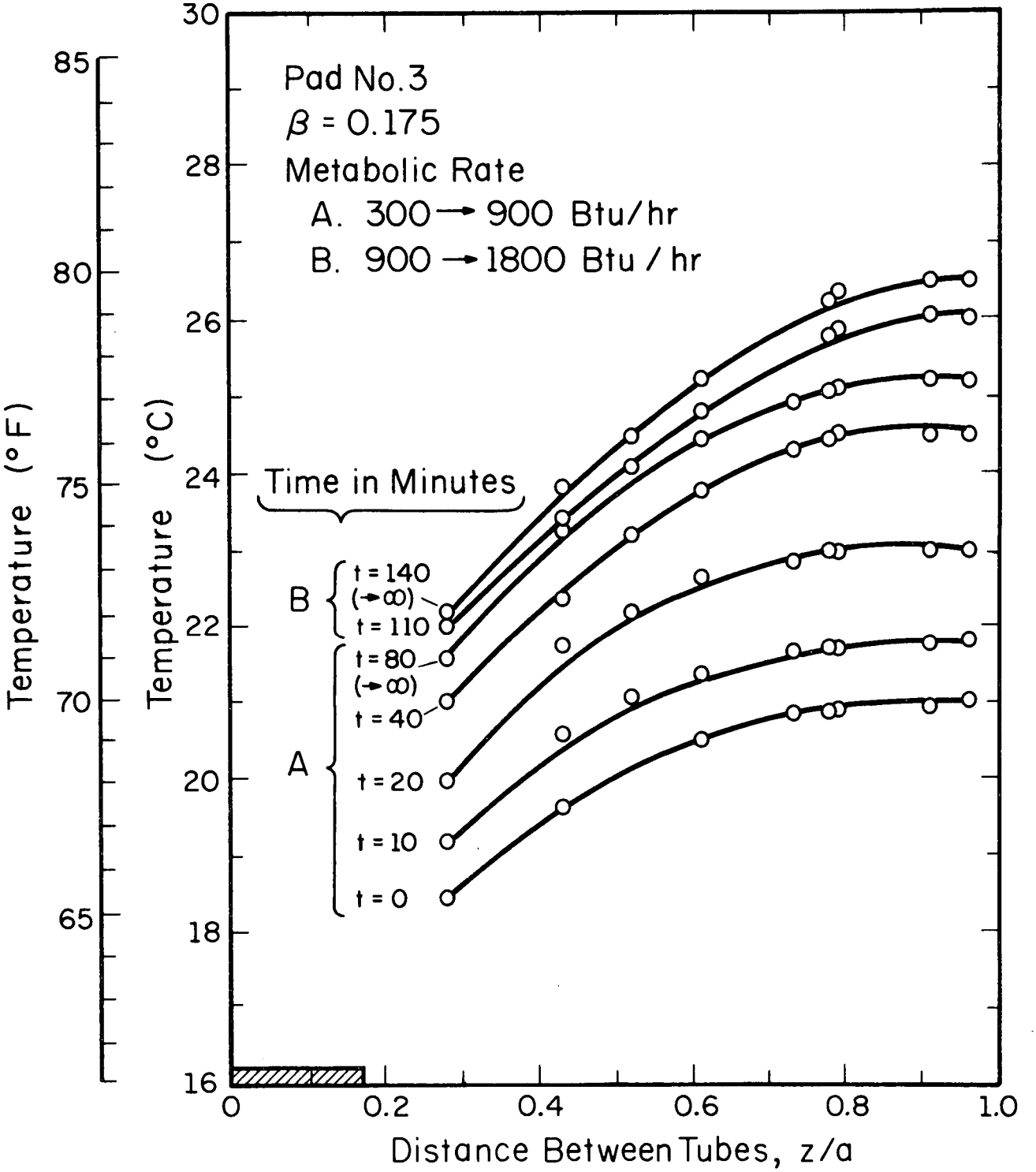

Figure 4.16 Development of temperature profile on the skin for pad No. 3 resulting from increases in metabolic rates from 300 to 900 Btu/hr (88 to 264 w) and from 900 to 1800 Btu/hr (264 to 528 w).

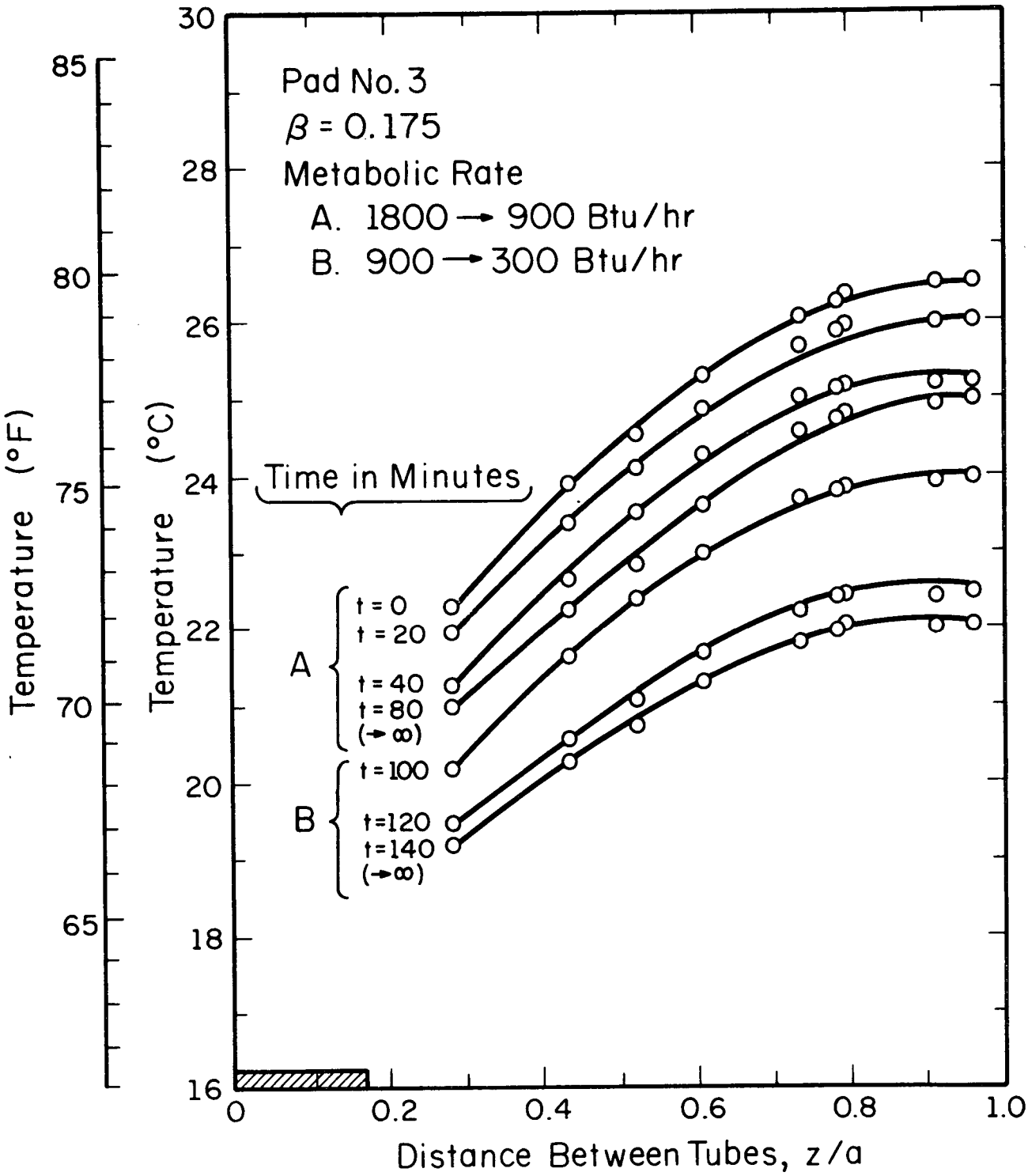

Figure 4.17 Development of temperature profile on the skin for pad No. 3 resulting from decreases in metabolic rates from 1800 to 900 Btu/hr (528 to 264 w) and from 900 to 300 Btu/hr (264 to 88 w).

In response to a decrease in metabolic activity, it was noted that pad No. 3 required 80 minutes to reach steady state, whereas pad No. 2 required only 40 minutes to reach the same level.

For the transition from 900 Btu/hr (264 w) to 300 Btu/hr (88 w), it can be seen that pad No. 3 required less time (60 minutes) than did pad No. 2 which required 80 minutes to reach steady state. It should be noted, however (see Fig. 4.15), that, in the case of pad No. 2, the lowest temperature was reached in approximately 40 minutes. During the remaining 40 minutes of the development of the steady state temperature profile, only the middle or warmer portion of the distribution was affected.

Again, some general comments can be made with respect to pad No. 2 in that it provided a lower, more uniform temperature distribution than did pad No. 3. Also, there was less of a range of temperature variation in the case of pad No. 2 as compared with pad No. 3. All of these observations can be accounted for by the higher tube density of pad No. 2 and the corresponding increase in cooling effectiveness.

5. SUMMARY AND CONCLUSIONS

Three separate cooling pads with different cooling tube sizes and spacings were constructed and tested. These pads were equipped with thermocouples and were used to measure the temperature profiles on the skin surface of the right thigh between adjacent cooling tubes. All pads were tested under the same experimental conditions with equal coolant flow rate and temperature. Pad No. 2 which consisted of 5/32 in. tubes spaced at 5/8 in. intervals provided the best cooling capacity. Pad No. 2 removed 15 percent of the total heat generated at high metabolic rates and much higher percentages at low metabolic rates. Pad No. 2 provided the lowest and most uniform skin temperature profiles throughout the tests. Also, the temperature profiles on the skin did not shift as much with changes in metabolic rate for pad No. 2 than with pads No. 1 and 3. The time constants for surface temperatures associated with changes in metabolic rate were also smallest for pad No. 2. In general, it can be concluded that pad No. 2 provided a lower, much more uniform and stable temperature distribution on the skin surface than was attainable with pads No. 1 and 3.

Times required for reaching a steady state from the onset of a change in activity level were also recorded. When an increase in metabolic rate was introduced, the times involved were found to be between 40 to 60 minutes, the shorter periods pertaining to pad No. 2 with the higher density of tubes. When the change in activity level was reversed, i.e., high (1800 Btu/hr, 528 w) to low (300 Btu/hr, 88 w), times for reaching a steady state temperature profile were about equal for pads No. 2 and 3 at 120 minutes. Thus, a ratio of

about 2-3 was found between the lengths of time required for the development of temperature profiles for extreme, opposite changes in levels of activity. When intermediate changes were used (experiments 9 and 10), the ratios of transient times were found to be of the order of 1-1.5. Overall transient times for these double-step changes were of the same order (~ 140 min) for both increasing and decreasing metabolic rates.

It is clear that both tube size and spacing have a noticeable effect on overall cooling efficiency. In order to optimize the relationship between these two parameters then, a definition of maximum metabolic rate should be secured. Once obtained, a cooling pad can be designed that will remove heat from the body at any predetermined rate.

A time dependent analytical solution has been obtained for the biothermal model in cylindrical coordinates. Equation (2.18) is the solution as a function of r, z, and t and was used to predict the transient temperature distributions on the skin surface between adjacent cooling tubes and for the one-dimensional geometry (uniform cooling of the skin).

A comparison between steady state measured and analytical results was attempted. The comparison was made with both the cylindrical and rectangular models of Ref. [1]. Agreement between measured and predicted results was found to be fair, particularly for pad No. 2. Improved techniques for measuring skin temperatures and physiological quantities, e.g., blood perfusion and metabolic heat generation rates, are required to render the comparison more meaningful and reliable.

REFERENCES

1. Shitzer, A., Chato, J. C. and Hertig, B. A., "A Study of the Thermal Behavior of Living Biological Tissue with Application to Thermal Control of Protective Suits," University of Illinois Technical Report, No. ME-TR-207, January 1971.

2. Nunneley, S. A., "Water Cooled Garments: A Review," Space Life Sciences, 2, 1970, pp. 335-360.

3. Burton, D. R. and Collier, L., "The Development of Water Conditioned Suits," Technical Note ME-400, Royal Aircraft Establishment, Farnborough, England, 1964.

4. Chambers, A. B., "Controlling Thermal Comfort in the EVA Space Suit," ASHRAE J., March 1970, pp. 33-38.

5. Waligora, J. S. and Michel, E. L., "Application of Conductive Cooling for Working Men in a Thermally Isolated Environment," Aerospace Medicine, 39, pp. 485-487, 1968.

6. Allen, J. R., "The Liquid Conditioned Suit, a Physiological Assessment," Memo 234, Flying Personnel Research Committee, Royal Air Force Institute of Aviation Medicine, Farnborough, England, 1966.

7. Chato, J. C., Hertig, B. A., et al., "Physiological and Engineering Study of Advanced Thermoregulatory Systems for Extra Vehicular Space Suits," Semiannual Report No. 2, NASA Grant No. NGR 14-005-103, June 1968.

8. Crocker, J. F., Webb, P. and Jennings, D. C., "Metabolic Heat Balances in Working Men Wearing Liquid Cooled Sealed Clothing," AIAA-NASA Third Manned Spacecraft Meeting, AIAA Publication CP-10, 1964, pp. 111-117.

9. Jennings, D. C., "Water Cooled Space Suit," J. Spacecraft, August 1966, pp. 1251-1256.

10. Allen, J. R., "Protection of Air Crews Against Heat," paper presented to Ergonomics Research Society Annual Conference, 1970.

11. Veghte, J. H., "Efficiency of Pressure Suit Cooling Systems in Hot Environments," Aerospace Medicine, 36, 1965, pp. 964-967.

12. Santa Maria, L.J., "Physiological Effects of Water Cooling under Different Environmental Conditions," Portable Life Support Systems, NASA SP-234, 1970, pp. 211- 220.

13. Webb, P. and Annis, J. R., "Cooling Required to Suppress Sweating During Work," J. Applied Physiology, 25, 1968, pp. 489-493.

14. Champaign-Urbana Courier, an Associated Press News Article, March 2, 1971.

15. Chato, J. C., and Shitzer, A., "Thermal Modeling of the Human Body--Further Solutions of the Steady-State Heat Equation," AIAA Journal, Vol. 9, 1971, pp. 865-869.

16. Pennes, H. H., "Analysis of Tissue and Arterial Blood Temperature in the Resting Human Forearm," J. of Applied Physiology, Vol. 1, 1948, pp. 93-122.

17. Hertzman, A. B., "Some Relations between Skin Temperature and Blood Flow," American Journal of Physical Medicine, Vol. 32, 1953, pp. 233-251.

18. Wissler, E. H., "Steady State Temperature Distribution in Man," J. of Applied Physiology, Vol. 16, 1961, pp. 734-740.

19. Perl, W., "Heat and Matter Distribution in Body Tissues and the Determination of Tissue Blood Flow by Local Clearance Methods," J. of Theoretical Biology, Vol. 2, 1962, pp. 201-235.

20. Chato, J. C., "A Method for the Measurement of Thermal Properties of Biological Materials," Thermal Problems in Biotechnology, ASME Symposium Series, 1968, pp. 16-25.

21. Trezek, G. J. and Cooper, T. E., "Analytical Determination of Cylindrical Source Temperature Fields and Their Relation to Thermal Diffusivity of Brain Tissue," Thermal Problems in Biotechnology, ASME Symposium Series, 1968, pp. 1-15.

22. Keller, K. H. and Seiler, L., "An Analysis of Peripheral Heat Transfer in Humans," Simulation Council Meeting, Chicago, Ill., March 9-10, 1970.

23. Grollman, S., The Human Body--Its Structure and Physiology, Second Edition, The Macmillan Co., London, England, 1969, p. 166.

24. Johnson, R. E., Robbins, F., Schilke, R., Mole, P., Harris, J. and Wakat, D., "A Versatile System for the Measurement of Oxygen Consumption in a Man," J. of Applied Physiology, Vol. 22, 1967, pp. 377-379.

25. Molnar, S., "The Relationship between Cardiac Time Components, Maximal Oxygen Consumption and Endurance Performance," University of Illinois at Urbana-Champaign, Ph.D. Thesis, 1970.

26. Consolazio, F. C., Johnson, R. E. and Pecora, L. J., Physiological Measurements of Metabolic Functions in Man, McGraw-Hill Book Co., New York, 1963.

27. Carpenter, T. M., Tables, Factors and Formulas for Computing Respiratory Exchange and Biological Transformation of Energy, Third Edition, Carnegie Institute of Washington, Washington, D.C., 1939.